OPTIMIZATION OF CARBON NANOTUBE PROPERTIES BY CONTROLLED AMOUNT OXIDIZERS

A Thesis Submitted to
the Graduate School of Engineering and Sciences of
İzmir Institute of Technology
in Partial Fulfillment of the Requirements for the Degree of

MASTER OF SCIENCE

in Physics

by

Deniz SÖYLEV

July 2011
İZMİR

We approve the thesis of **Deniz SÖYLEV**

_____
Assist. Prof. Dr. Yusuf SELAMET
Supervisor

_____
Assoc. Prof. Dr. Salih OKUR
Committee Member

_____
Assist. Prof. Dr. Ömer MERMER
Committee Member

5 July 2011

_____
Prof. Dr. Nejat BULUT
Head of the Department of Physics

_____
Prof. Dr. Durmuş Ali DEMİR
Dean of the Graduate School of Engineering and Sciences

ACKNOWLEDGEMENTS

I would like to express my gratitude to all those who gave me the help to complete this thesis. Firstly, I thank my supervisor Assist Prof Yusuf Selamet for his invaluable support during the thesis study. Also, I thank Assist Prof Dr Süleyman Tari for growing our catalyst thin films in his lab whenever we need. Moreover I thankfully acknowledge TUBITAK for financial support during this project (TUBITAK-109T534). Furthermore I am very thankful to my lab mates at Carbon Nanostructure Laboratory Atike İnce, Gülay Bülbül, Elif Özçeri for their warm friendship and help. Personally, my special thanks go to some special people Saadet Çolak, Yasemin Nefise Aydın and Esra Yılmaz for their good heart and love and I feel very lucky to have them in my life. Finally, I am very thankful to my family for their financial support, comments and motivation in all my life.

ABSTRACT

OPTIMIZATION OF CARBON NANOTUBE PROPERTIES BY CONTROLLED AMOUNT OXIDIZERS

This thesis work focuses on growing high quality carbon nanotubes using ethylene as hydrocarbon gas in thermal chemical vapor deposition method in presence of weak oxidizers. We carried out experiments to study the ratio of amount of CO_2, O_2 and H_2O in pretreatment to growth and the timing of the metal-oxide to metal conversion in presence of the oxidizers.

Firstly, the effects of CO_2 addition were investigated on a variety of growth conditions to study the controlled diameter growth of CNTs. The main growth parameters controlled in this work in the CNT growth were CO_2 level, pretreatment time and temperature. Pretreatment times of 15, 10, 5, 2 minutes were studied. CO_2 flow rates were send in system during both pretreatment time and growth time at 10:1, 10:2, 5:1, 5:2, 2:1 and 2:2 sccm ratios, respectively. We also studied two different growth temperatures at 740 ^{o}C and 760 ^{o}C.

Secondly, the influence of O_2 for effective CNT growth was investigated by utilizing different pretreatment times and O_2 levels. Pretreatment times of 15, 10, 5, 2 minutes were studied. O_2 gas flow rates during pretreatment time and growth time were studied as 5:1, 5:2, 2:2, 2:1, 2:0.5, respectively. As a result, we obtained small diameters with the pretreatment time of 15 min. in the presence of O_2.

Thirdly, the effects of H_2O vapor for effective CNT growth on $Fe/Al_2O_3/SiO_2$ were examined. During the experiments, pretreatment time was kept at a constant value of 15 min. and H_2O vapor content in Ar was varied. The results of examined analyses show that the best results were obtained at the growth 60 ^{o}C (A) / 60 ^{o}C (A).

Finally, all data were subjected through a statistical analysis. From this study we have seen that the majority of the samples had Log-Normal diameter distributions by adjusting oxidizer amount and pretreatment timing. We were able to control CNT diameters within very narrow diameter ranges.

ÖZET

KARBON NANOTÜP ÖZELLİKLERİNİN KONTROLLÜ MİKTAR OKSİTLEYİCİLERLE İYİLEŞTİRİLMESİ

Bu tez çalışması, etilen gazı termal kimyasal buhar biriktirme tekniği ile zayıf oksitleyiciler varlığında yüksek kalitede karbon nanotüplerin sentezlenmesine odaklandı. Kullanılan oksitleyicilerin, CO_2, O_2, H_2O, akış oranları ve metal oksitten metal forma dönüşüm zamanını çalışmak için deneyler gerçekleştirildi.

İlk olarak CO_2 etkileri CNT' lerin kontrollü çap büyümesini çalışmak için farklı büyüme koşullarında çalışıldı. Bu çalışmada CNT büyümesinde ana büyütme parametreleri CO_2 akış oranları, ön işlem süresi ve sıcaklıktır. Burada 15, 10, 5, 2 dakikalık ön işlem süreleri çalışıldı. Ayrıca CO_2 gaz akış oranları hem ön işlem süresi hem de büyüme süresi boyunca sırasıyla 10: 1, 10: 2, 5: 1, 5: 2, 2: 1 and 2: 2 sccm olarak gönderildi. Diğer çalışılan parametre olan sıcaklık değerleri 740 ^oC and 760 ^oC.

İkinci olarak aynı şekilde etilen CVD tekniği kulanılarak $Fe/Al_2O_3/SiO_2$ üzerine etkili CNT büyütmek için sisteme farklı miktarlarda O_2 gönderilerek ve farklı ön işlem süreleri etkileri araştırıldı. Ön işlem süreleri 15, 10, 5, 2 dakika olarak çalışıldı. O_2 gaz akış oranları hem ön işlem hemde büyüme sırası boyunca sırasıyla 5:1, 5:2, 2:2, 2:1, 2:0.5 sccm olarak çalışıldı. Sonuç olarak, 15 dakikalık ön işlem süresi boyunca küçük çaplar elde ettik.

Üçüncü olarak, CVD sistemine H_2O göndererek $Fe/Al_2O_3/SiO_2$ ince film üzerine etkili CNT büyümesi incelendi. Deneyler sadece su buharının etkileri çalışıldı. Tüm deneyler boyunca önişlem süresi 15 dakika olarak çalışıldı ve sadece su buharının miktarları değiştirildi. En iyi sonuçlar 60 ^{o}C (A) / 60 ^{o}C (A) seviyelerinde elde edildi.

Son olarak, tüm örnekler kapsamlı şekilde istatiksel analiz edildi. Bu çalışmada örneklerin çoğunun çap dağılımları Log-Normal dağılım göstermektedir. Çok dar aralıklarda CNT çapları elde edebildik.

TABLE OF CONTENTS

LIST OF FIGURES

Figure **Page**

LIST OF TABLES

CHAPTER 1

INTRODUCTION

Carbon nanotubes (CNTs) are a new form of carbon discovered in 1991 by Sumio Iijima, a microscopist at the NEC Corporation laboratory in Tsukuba, Japan. Since their discovery, CNTs have become the subject of intense scientific study due to their extraordinary properties. In order to determine their growth mechanism there are large number of experiments conducted and great number of papers published. However, the growth mechanism and dynamics do still not clearly known.

A single wall carbon nanotubes (SWNT) is a graphene sheet rolled into a cylinder, with the ends closed off by caps of various shapes. CNTs have excellent physical properties, due to sp^2 hybrid bonding, the size of these materials and atomic structure, such as high aspect ratio, high Young modulus, high tensile strenght, high thermal and electrical conductivity (Salvetat, et al. 1999). Some of the rapidly growing applications include field emission device, scanning microscopy probe, sensors, high strength composite and supercapacitors (Futaba, et al. 2006).

The CNTs are classified as SWNT and multiwall nanotubes (MWNT) (Dresselhaus, et al. 2001). The types of CNTs can be determined by chirality vector ($C=n\hat{a}_1+m\hat{a}_2$) and n, m (n and m defining the CNT structure). The chirality vector gives information about the electronic structure, since depending on chirality a SW. CNT can be a semiconductor or a metal (Dresselhaus, et al. 2004). Hence, the (n,m) values indicate whether the SWNT is metalic or not. If (n-m)=3q, this nanotube is metalic and if (n-m)=3q+1, this nanotube is semiconductor, where q is an integer (Thostenson, et al. 2001). If n=m and $\theta=0^o$, this nanotube corresponds to armchair type, m=0 corresponds to zigzag type CNT at $\theta=30^o$, and if $n\neq m$ the tube is chiral and chiral angle is between 0^o and 30^o (Belin and Epron 2005). All armchair nanotubes are metallic nanotubes, but zigzag nanotubes are either semiconductor or metallic nanotubes (Saito, et al. 1992).

CHAPTER 2

CARBON NANOTUBES

2.1. Carbon Structures

Carbon is one of the elements that have covalent bonds to become stable. A covalent bond is one in which one or more electrons are shared between atoms. The carbon atom has six electrons, two in its inner shell and four in its outer shell. There are many allotropes of carbon such as graphite, diamond, carbon fibers, fullerenes, and carbon nanotubes.

Diamond is an allotrope of carbon, where the carbon atoms are arranged in a variation of the face-centered cubic crystal structure. Diamond is renowned as a material with superior physical qualities, most of which originate from the strong covalent bonding between its atoms. In particular, diamond has the highest hardness and thermal conductivity of any bulk material. These properties determine the major industrial application of diamond in cutting and polishing tools. Diamond structure is shown in Figure 2.1.

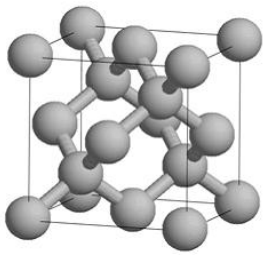

Figure 2.1. Diamond in the cubic structure
(Source: Stahl 2000)

Graphite is a layered and planar structure that the carbon atoms are arranged in a hexagonal lattice with separation of 0.142 nm in each layer, and the distance between planes is 0.335 nm. Graphite is an electrical conductor and it is chemically more reactive than diamond. Figure 2.2 shows the structure of graphite. A single atomic plane of graphite is called graphene layer which has remarkable electrical, thermal, and physical properties.

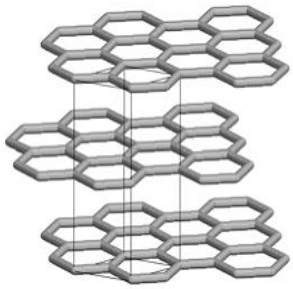

Figure 2.2. The structure of graphite
(Source: Stahl 2000)

One of another allotropes of carbon is fullerene discovered in 1985 (Kroto, et al.1985). Fullerene can contain 60, 70 or 82 carbon atoms and has a hollow closed sphere and ellipsoid structure. That is, they are closed spheres composed of pentagons and hexagons. C_{60} molecule is named as Buckyminster fullerene.

Fullerene has the form of a hollow closed sphere or ellipsoid and can consist of 60, 70 or 82 carbon atoms. In the fullerene structure carbon atoms bonded to one another with both hexagon and pentagon rings. C_{60} molecule is a small fullerene molecule in which no two pentagons share an edge and as shown in Figure 2.3.

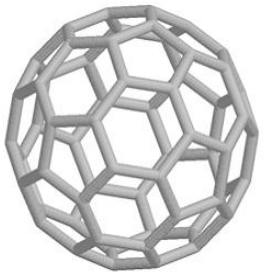

Figure 2.3. C60 Buckminsterfullerene
(Source: Stahl 2000)

The last one is carbon nanotube which is going to be described in the following step as the subject of this study.

2.2. Carbon Nanotubes

2.2.1. Discovery

Carbon nanotubes become a form of cylindrical tubes of a graphite layer with nanometer size diameters. In 1950, electron microscopes were becoming popular in wide range of research field. The first tube-shaped hollow structure of carbon was discovered by Radushkevich ve Lucyanovich, Russian researchers, with an electron microscope in 1952 (Radushkevich, et al. 1952). However, this publication did not attract much interest because language publication was in Russian. In 1972 R. T. K. Baker worked on stone forms of nested carbon filaments with TEM and growth mechanism of these related to diffusion in metal particle of carbon (Baker, et al. 1972). In 1976 Oberlain and Endo mentioned only one cylinder hubs in graphite structure of carbon fibers (Oberlin, et al. 1976). In 1991 Sumio Iijima, an expert of electron microscopy, realized the tubular structure of carbon during investigations on the fullerenes, which is another structure of carbon (Dupuis 2005). Single wall carbon nanotube tube was grown by two different techniques (chemical vapor deposition and arc discharge technique) at the same time about two years later from these studies (Iijima, et al. 1993; Bethune, et al. 1993). The number of nested graphite walls around the same center determines the types of tubes.

2.2.2. Types of Carbon Nanotubes

Type of carbon nanotube is determined by the number of the concentric graphene layers. Carbon nanotubes are clasified as single wall carbon nanotubes and multi wall carbon nanotubes. If carbon nanotube contains one graphene layer, it is named single wall nanotube (SWNT); whereas if it contains two or more concentric layer, it is named multi wall carbon nanotube (MWNT).

2.2.2.1. Single Wall Carbon Nanotube

A single wall nanotubes (SWNT) is occurred by a graphene sheet rolled into a cylindir with a diameter of about 0.4-10 nm and lengths from microns to cm.

A single-wall carbon nanotube (SWNT) is defined by a graphene sheet rolled into a cylindrical shape with a diameter of about 0.4-10 nm and lengths extending up to several microns. The shape of a SWNT is shown in Figure 2.4. If we ignore two ends of carbon nanotube and focus on the large aspect ratio of the tube, carbon nanotubes can be considered as one-dimensional nanostructures with axial symmetry and they have excellent properties because of this symmetry (Baddour, et al. 2005). A single wall carbon nanotube can be metallic or semiconductor.

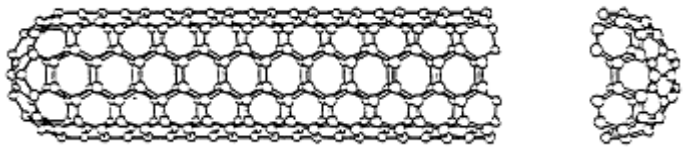

Figure 2.4. An illustration of a SWNT
(Source: Dresselhaus 1998)

2.2.2.2. Multi-Walled Carbon Nanotubes

CNTs with more than one concentric graphene cylinders coaxially arranged around a central hollow with a constant interlayer distance which is nearly equal to 0.34 nm is called multi-wall carbon nanotube (Dresselhaus, et al. 2001). MWNTs are stronger than SWNTs although they have more defects than SWNTs (Dai 2002). Graphite layers easily seperated from each other due to weak vander Waals forces between planes, but seperation of cylinders of MWNT from each other is difficult. The investigation of physical properties of MWNTs is more difficult because of the difficulty of making measurements on the indivudual shells of the nanotube. The shape of a MWNT is shown in Figure 2.5.

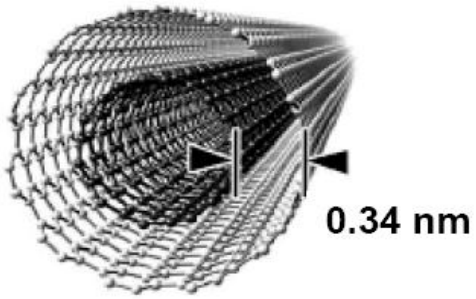

Figure 2.5. An illustration of a MWNT
(Source: Iijima 1999)

2.2.3. Classification of Carbon Nanotubes

According to the direction of the hexagons which are the six membered carbon rings, the structure of CNTs can be classified in three different configurations such as armchair, zigzag and, finally, chiral carbon nanotube (Dresselhaus, et al. 2001). In Figure 2.6 the formations of three different nanotubes are indicated.

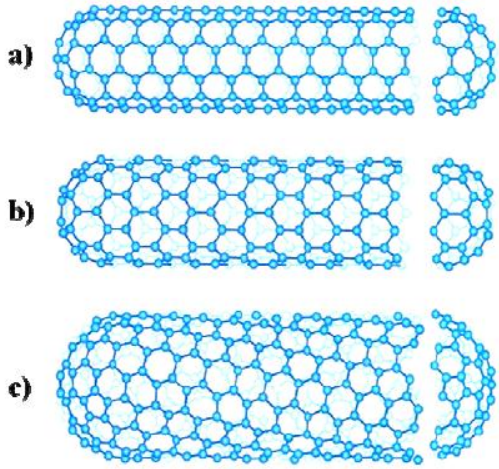

Figure 2.6. Classification of CNTs, a) Arm-chair, b) Zig-zag, c) Chiral CNTs
(Source: Dresselhaus, et al. 2001)

The type of a carbon nanotube is determined by its chiral vector ($C_h = n\hat{a}_1 + m\hat{a}_2$) and its chiral angle (θ) (Reich, et al. 2004). The chiral angle (θ), being the angle between C_h and $\hat{a}_1$ is measured relative to the direction defined by $\hat{a}_1$ (Rotkin and Subramoney 2005). This angle has values in the range of $0 \leq \theta \leq 30$. These two parameters can be seen in Figure 2.7.

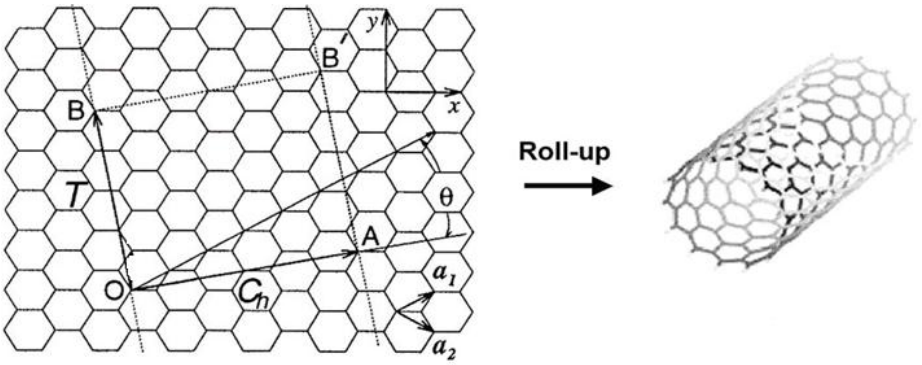

Figure 2.7. An illustration of rolling graphene sheet into a tube
(Source: Saito, et al. 1998)

If n=m and $\theta=0^o$, this nanotube corresponds to armchair type, m=0 corresponds to zigzag type CNT at $\theta=30^o$, and if n≠m the tube is chiral and chiral angle is between 0^o and 30^o (Belin and Epron 2005). According to depending on the tube chirality, the electrical properties of the CNTs differ from one another; CNTs can be either metallic or semiconducting; if n-m=3q, where q is an integer, the CNTs are metallic; while n-m≠3q, the CNTs are semiconducting (Ivchenko and Spivak 2002). The armchair nanotubes indicated by (n,n) are always metallic if n is a multiple of 3, and the zigzag nanotubes (n,0) also are metallic. Figure 2.8 shows that carbon nanotubes are either metallic or semiconducting. The encircled dots are the metallic nanotubes, the small dots are the semiconducting nanotubes.

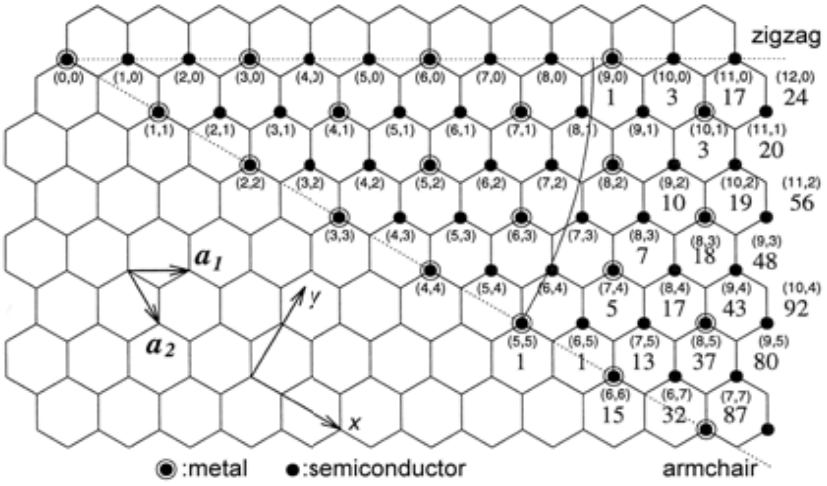

Figure 2.8. Possible vector images with the pairs of integer (n,m) for general CNTs
(Source: Dresselhaus, et al. 1993)

2.3. Carbon Nanotube Synthesis Methods

Three main growth techniques for carbon nanotubes are widely used. One of these is arc discharge technique being the first synthesizing technique of tubes, the second one is laser evaporation technique and the last one is chemical vapor deposition technique. These three methods have some advantages and disadvantages as shown in Table 2.1. Each technique will be shortly explained below.

Table 2.1. Advantages and disadvantages of three main techniques used for the CNT growth

Growth methods	Advantages	Disadvantages
Arc-discharge	• the high growth rate • controlled experimental conditions	• impurity • expensive equipment • low yield • difficult reproducibility
Laser Ablation	• less structural defects • narrow diameter range	• high-temperature production • expensive equipment • low yield
CVD	• simple mechanism • low cost • low-temperature production • high yield • high alignment CNTs • growth control • different buffers layers	• impurity • high structural defects

2.3.1. Arc-Discharge Method

This technique is the first growth technique to achive carbon nanotubes growth (Iijima 1991). This method is related to the CNT growing on carbon electrodes by applying DC (direct current) between two graphite electrodes during arc-discharce evaporation of carbon in argon or helium atmosphere (Popov 2004). In Figure 2.9 a schematic illustration of the arc-discharge setup is shown.

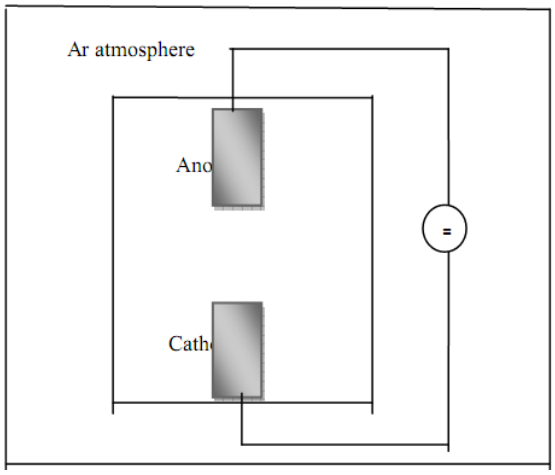

Figure 2.9. Simple schematic illustration of an arc generator
(Source: Popov 2004)

In addition, there are two high-purity graphite electrodes in this method. A graphite electrode can contain catalyst such as Fe, Co, Ni, and it is the anode; the other one is used as a cathode (Iijima, et al. 1993). A voltage of 20-40 V and a dc electric current of nearly 50-100 A are applied between the electrodes. When current is applied, temperature reaches to about 4000 ^{o}C and it causes anode to vaporize and condense on cathode surface where nano particles grow. Both electrodes are cooled with water during the process, and the arc is generally operated in He atmosphere at low pressure between 50-700 mbar. Carbon nanotube synthesis can be done with or without catalyst by the arc discharge method in order to produce multi-wall carbon nanotubes and single-wall carbon nanotubes, respectively (Journet and Bernier 1998).

This technique can have very high growth rate (10 m/s), but length of CNTs is about 1μm due to the short arc duration. Yield and quality are very low and there is impurity problem.

2.3.2. The Laser Ablation Method

In 1995 the group of Guo used this method to produce CNTs (Guo, et al. 1995). Laser ablation method works with the same principle as arc-discharge method, that is initial evaporation of carbon gas followed by condensation on electrodes cooled with water (Rasmussen 2005). The furnace is heated at high temperature nearly 1200 ^{o}C and an inert gas such as argon or helium passes through the tube. At this high temperature, a pulsed laser is used to vaporise the graphite target which is located in the center of quartz tube furnace to produce fullerenes and CNTs. The target can contain a mixture of graphite and metal catalysts such as Fe, Co and Ni (Yudasaka, et al. 1999; Kataura, et al. 2000). In Figure 2.10 a schematic illustration of the laser ablation setup is shown.

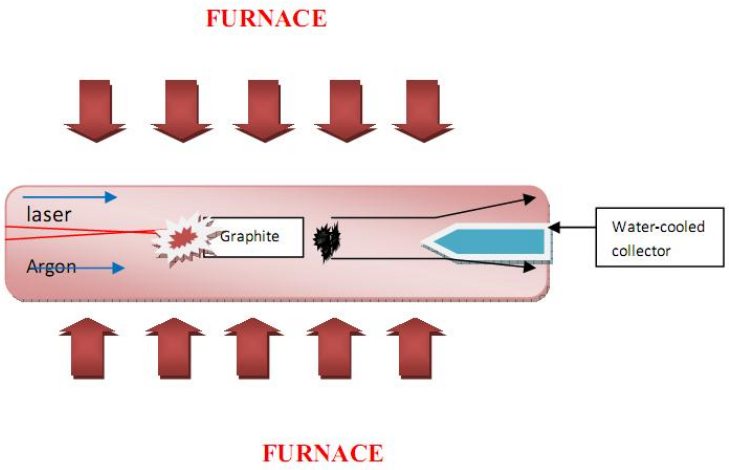

Figure 2.10. Schematic illustration of a laser ablation technique
(Source: Guo, et al. 1995)

Graphite target may also include elements of Fe, Co, and Ni. This technique can grow very high-quality CNT. However, the length of CNTs can also remain around 1 μ m and the growth rate is very low.

2.3.3. Chemical Vapor Deposition Method

Chemical vapor deposition technique was used in making carbon fibers up to this time from 1959 (Walker, et al. 1959), but the first carbon nanotubes synthesis was realized in 1993 (Dai 2002). There are many different CVD techniques for carbon

nanotube growth such as plasma enhanced CVD, thermal CVD, alcahol catalytic CVD, laser assisted CVD and aero-gel supported CVD. Thermal CVD method will be explained below in details.

There are two main steps for carbon nanotube growth; the first one is the catalyst preparation and the second one is the nanotube growth on this prepared catalyst. A thin film layer can be converted by annealing to nanocatalyst particles, or a catalyst can be synhesized by some chemical methods. Initially, the prepared sample is placed in a quartz tube and then this quartz tube is palced in furnace. The temperature of furnace is set to a selected point. During the rise of the temperature to the set point, an inert gas flows through the tube to prevent the oxidation of samples. When the furnace reaches to the selective temperature, an annealing can be done with H_2 or NH_3 to reduce catalyst nano particle from oxide form to metal form (Lee and Park 2001).

The other step is sending hydocarbon gas the system for decomposition of gas molecules on the catalyst surface which is followed by carbon deposition onto the catalyst. After that, the carbon precipitates to form cabon nanotubes because carbon has a low solubility in these metals at high temperature. These hydrocarbon gases such as CH_4, C_2H_4, C_2H_2 and C_6H_6 can be used as a carbon source (Cui, et al. 2003).

CVD is the most common method to grow carbon nanotubes because CVD has many advantages compared with the other two methods. Firstly, this method is performed at low temperature compare to other growth methods (Reich, et al. 2004) and also the diameters of CNTs can be controlled by controlling size of catalyst nanoparticles (Weifeng, et al. 2003). The other advantage is easy to perform CVD process and inexpensive technique for synthesis of carbon nanotubes. In addition, more than one sample can be grown at a time. This method is adaptable for large scale production of nanotube metarials (Yamacan, et al. 1993; Weifeng, et al. 2003). The schematic illustration of a thermal CVD system is shown in Figure 2.11.

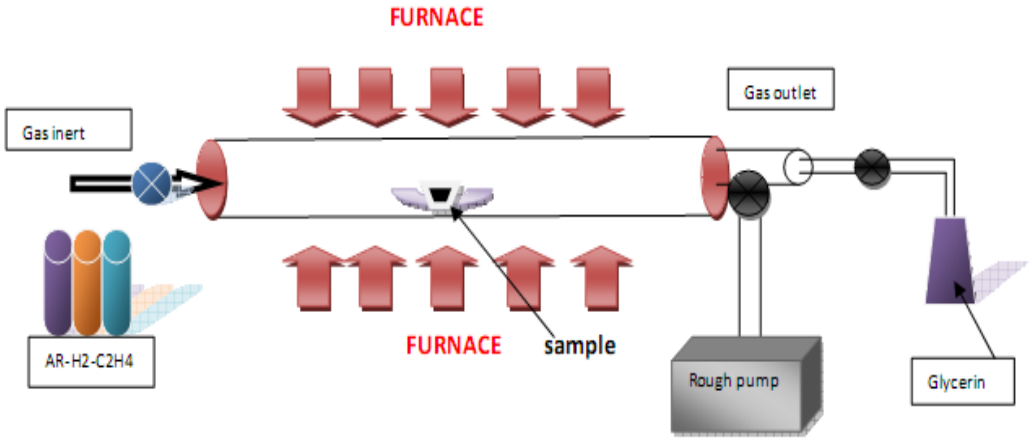

Figure 2.11. A schematic illustration of a CVD System
(Source: Journet and Barnier 1998)

CNTs can grow in either base growth or tip growth mechanisms. The first growth is called as the base growth in which the metal catalyst particle stay at the end of the tube. The other growth type is called as the tip growth in which the metal catalyst particle might be removed from the surface and moves at the top of the growing carbon nanotube (Saito, et al. 1994). The types of growth mechanisms are illustrated in Figure 2.12.

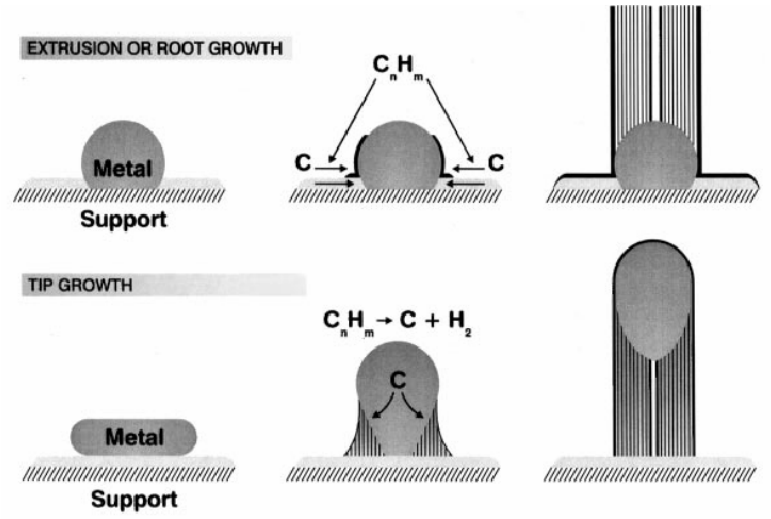

Figure 2.12. Schematic illustrations of carbon nanotube growth mechanisms a) Base or root growth, b) tip growth (Source: Sinnot, et al. 1999)

CHAPTER 3

THE CATALYST

3.1. Catalyst Thin Film

There have been many parameters affecting the growth of CNTs. One of the most significant parameters affecting the CNT growth is the catalyst material. A catalyst is described as a susbtance that increases the rate at which a chemical reaction approaches equilibrium without itself becoming permanently involved in the reaction in general chemistry (Richardson 1989). Transition metal particles in periodic table are generally used in CNT growth either in metallic or oxide forms. Transition metals possess some suitable properties such as low melting temperature, equilibrium vapor pressure, solubility of carbon and carbon diffusion rate in the metal for CNT production. The most significant property of the metals related to CNT formation is their ability to catalytically decompose gaseous carbon-containing molecules (Moisala, et al. 2003).

Much research has been done into determine the most suitable catalyst material. La, Cu, Gd, MgO, Ni, Co, Fe, Pd, Cr, Mn, Zn, Cd, Ti and Zr have been used for this research and the common catalyst materials used for the CNT growth are Fe, Co, and Ni in the literature. The type of catalyst on which CNT can grow, is named succesful catalyst; otherwise, it is named unsuccesful catalyst. These metals (Fe, Co, Ni) have finite carbon solubility at high temperatures (Dai 2002; Park, et al. 2002). The carbon solubility limit of succesful catalyst is between 0.5wt%-1.5wt% and if the carbon solubility is very close to zero and the metal carbides prevent the growth of CNTs, these catalyst are unsuccesful (Vecchio and Deck 2006).

The performances of these three catalyst materials were investigated according to their growth rate of CNTs which was on the order of Ni>Co>Fe (Lee, et al. 2002). The average diameter of CNTs follows the sequence of Fe>Co>Ni catalysts (Lee, et al. 2002). The success of these metals was suggested to relate to the catalytic activity for decomposition of carbon precursors, the formation of meta-stable carbides, the diffusion of carbons, and the formation of graphitic sheets (Kiang 2000).

When iron-based catalyst was used, many research groups observed CNT formation (Kukovecz, et al. 2000; Ermakova, et al. 2001; Pan , et al. 1999; Hernadi, et al. 1996; Fonseca, et al. 1996; Cui, et al. 2000; Wang , et al. 2001; Duesberg, et al. 2003; Klinke, et al. 2001; Ivanov, et al. 1994; Venegoni, et al. 2002; Fonseca, et al. 1996; Cho, et al. 2002). In Figure 3.1 the Fe catalyst particles are shown.

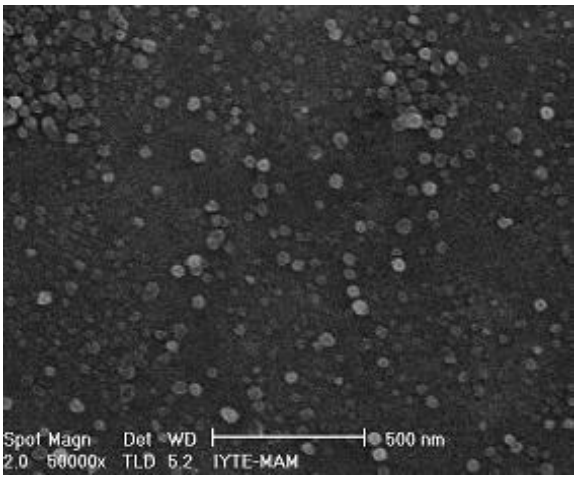

Figure 3.1. Fe catalyst particles imaged by SEM
(Source: Aksak, 2008)

3.2. Thin Film Support Layer

The support layer is significant for surface mobility of catalyst nanoparticle because the support layer affect the catalyst orientation and also the size of catalyst nanoparticles (Dai 2002).

The support layer type may have different interactions between the supporting material and the catalyst metal. The interaction between catalyst and support material directly affects the dispersion, morphology and size of catalyst nanoparticles (Qingwen, et al. 2002). Chemical or physical interactions can occur between support layer and catalyst metal. Van der Waals and electrostatic forces are the physical forces that prevent mobility of catalyst particles on the support surface. These forces also reduce thermally driven diffusion and metal particle sintering on the support material. Hence, controlled catalyst particle size is achieved during CNT sythesis (Moisala, et al. 2003). Chemical interactions also take place in the stabilization of size distribution of catalyst

particles. When chemical interaction is very strong, particle mobility decreases which prevents the particle coalescence.

The most effective support material is porous one to obtain a suitable size of catalyst nanoparticles for CNTs. High porousity support material with strong metal-support interactions and high surface areas produce SWNTs with better characteristics at a larger quantities. Strong support-metal interaction is significant, since it can prevent metal species from aggregating to form unwanted larger particles (Dai 2002).

The most common buffer layers are silica (SiO_2) and alumina (Al_2O_3). Al_2O_3 is better than SiO_2 as a support layer for hydrocarbon CVD proces although Al_2O_3 is an electrical insulator and has high termal conductivity (Gassell 1999).

3.3. Effect of Oxidizers on Catalyst

It is tempting to suggest that these oxidizers play a cleaning role by etching away amorphous carbon and, thus, maintaining high catalyst activity for CNT growth. Accordingly, it is the purpose of this study to understand the role of oxidizers during both pretreatment time and growth time. We carried out experiments to study the ratio of CO_2, O_2 and H_2O and the timing of the metal-oxide to metal conversion in presence of CO_2, O_2 and H_2O as oxidizers. Oxidizers was utilized during reduction pretreatment process to control the size of catalyst particle and during the growth process to prevent amorphous carbon formation on the outer walls of CNTs, to reactivate catalyst particle poisoned by amorphous carbon and to prevent further enlargement of catalyst particle.

3.3.1. Literature Search

Hata et al. observed that a small amount of H_2O vapour mixed in reaction during growth reduces amorphous carbon and results in more effective CNT production (Hata 2004). H_2O is essential ingredient for extending the lifetime of the catalyst during pretreatment duration and thus leading to effective CNT growth (Hata 2004).

Li et al. mentioned that the heights of CNTs grown with addition of air continue to grow up to 500 minutes. Also the study of Li et al. was mentioned that mean CNT diameters are 35 nm grown near buffer layer and up to 100 nm on the higher parts.

These diameters indicate that the growths have similar to carbon nano fiber structure rather than cylindrical CNT structure (Li 2008).

Huang et al. and Futuba et al. studied on effective CNT growth (Huang 2009; Futuba 2006). The study done by Huang in the presence of CO_2 was reported a formation of domed growth (short sides, bulky in the middle, almost hemisphere shape), height of CNT distribution is more uniform and converts to radial block figure. The structures such as dish (long sides and short middle) were obtained by increasing line heights with increased addition of CO_2. Morphological variation observed with the increase of amount of CO_2 was explained with the change of CNT growth velocity and change of bonding force between CNT and support, thus, maintaning a controlled CNT growth with the use of CO_2. Amounts of CO_2 (6.5 mol%-30.4 mol%) used in this study was greater than amount of CO_2 used for our oxidation study. CNTs at around of Fe particles in the high CO_2 ratio were mentioned to be dissociated via catalytic oxidation. It is mentioned not be very effective because CO_2 react with H_2 at low CO_2 concentration. In this study Raman G/D ratio was increasing with increased CO_2 concentration and density of SWNT increases up to 70% from 20% (Huang, et al. 2009).

As for the study done by Futuba et al., water vapor and other C and O included gases (CO_2, acetone, ethanol) remove amorphous carbon in catalyts particle poisoned. From these enhancers the best result was obtained with H_2O, however the worst result was obtained with CO_2. It was emphasized that carpet height arrays at some samples terminated after a few minute. CO_2 was utilized for the purpose of enhancing and the density.

Based upon the above explained results, CO_2 plays at least two important roles in the CNT synthesis. Firstly, CO_2 acts as an oxide source to remove the amorphous carbon, which would keep the catalyst active for a longer time and consequently increase the length and yield of tubes. Secondly, CO_2 can be dissociated on the surface of the catalyst clusters and reacts with other molecules and radicals, resulting in intermediates that can be more effective for the CNT growth. On the other hand, in our study oxidizers were utilized with purpose to control catalyst size and consequently to control CNT diameters. We did not aim for CNT enhancement. Additionally, diameter distributions were 2-3 nm in terms of standard deviation. These values were comparable diameter distribution of SWNT that Hata's group densely working in subject of growth enhancement.

CHAPTER 4

EXPERIMENTAL

This chapter give some main information about the experimental process. The first section of this chapter is focused on the catalyst film deposition process by DC magnetron sputtering. The second section offers a brief description of the thermal CVD. The third section covers the main growth steps of CNTs grown by TCVD method, and the following section is focused on characterization techniques which are SEM and Raman Spectroscopy.

4.1. DC Magnetron Sputtering Process

In this study, a DC magnetron sputtering method was utilized to deposit Fe catalyst film onto the $Al_2O_3/SiO_2/Si$ substrates. The growth system (AJA ATC Orion) is controlled by a computer and reaches very high vacuum levels. It has 2-inch magnetron heads including a substrate holder which is able to rotate at different speeds in order to have a uniform deposition, a heater, and a load-lock with a magnetic arm and a cylindrical stainless steel chamber. The targets are bonded to a water cooled copper carrier, ensuring both electrical and thermal contact. The distance between substrate and target was kept at 7 cm.

A typical growth substrate consists of $Fe/Al_2O_3/SiO_2$. Si wafers (100) with 2-inch diameter and a typical resistivity of 1-20 ohm-cm were purchased to be used as support layer. These silicon substrates were cleaned chemically in methanol for 15 min in an ultrasonic bath and rinsed with ultra-pure water for 15 min prior to growth. The commercial silicon films were first oxidized by dry thermal oxidation system. 10-15 nm thick alumina (Al_2O_3-barrier) and than 0.5–3 nm thick iron (Fe catalyst) layers were deposited on a silicon dioxide (SiO_2) wafer by DC magnetron sputtering. The magnetron sputtering chamber was evacuated to a pressure of 10^{-6} Torr and depositions were carried out at a rate of 0.1 A^o/s and 20 W, at a growth pressure of 0.5 mTorr.

4.2. Thermal Chemical Vapor Deposition Process

A thermal chemical vapor deposition (TCVD) apparatus was utilized for the growth of CNTs. The reactor consists of a horizontally mounted quartz tube with a diameter of 2.54 cm and a length of 60 cm, equipped with various gas lines and mass flow controllers. In order to achieve different heating ramp rates, furnace with programmable heater controller (Lindberg/Blue TF55035C Split Mini tube Furnace) was used. The mass flow of the gases was controlled electronically. The quartz boat is utilized for as a holder for the samples onto which the CNTs were grown. The furnace and the quatz boat are shown at Figure 4.1 and Figure 4.2, respectively. The quartz boat onto which the substrates were accommodated is placed in the middle of the furnace because it is an isothermal area. The upper temperature limit of the furnace is 1100 ^{o}C and it is lower than the melting temperature of quartz. The maximum temperature used in this study was 760 ^{o}C.

Figure 4.1. The TCVD system, CNL Lab in Physics Department IYTE

Figure 4.2. Quartz boat used to carry catalyst particles into furnace

In this study, all experiments for CNT growth were performed at atmospheric pressure. Firstly, the furnace is set to the desired temperature before the CNT growth, and the temperature is increased in an Ar ambient. Argon is used to purge the reactor while the CVD furnace was heated to desired temperature. Argon is also used as the carrier gas to carry the gases to the reaction chamber. After the desired temperature is reached, both etching gas (H_2) and oxidizers are sent into the system in order to form the catalyst nanoparticles. Both H_2 and oxidizers provide the reduction from metal oxide catalyst to metal catalyst which are more suitable for CNT growth. CO_2, O_2 and H_2O are used as the oxidizers during all experiments. When the pretreatment time finishes, C_2H_4 gas flow was started to initiate CNT growth. Ar, H_2, oxidizers continued to flow during CNT growth. . The total gas flow was 250 sccm at growth. Different gas flow rates and pretreatment time for oxidizers were investigated. Other gas flows are constant during all experiments. The flow rates of other gases are 150 sccm Ar gas, 140 sccm hydrogen gases and 180 sccm C_2H_4 gases. Growth time is also another parameter for CNTs, in this study the growth time is 15 minutes for all of the experiments. This parameter affects the length of CNTs, not the growth mechanism so 15 minutes is enough for this study. When the growth time is finished, firstly the hydrocarbon gas is turned off and then both the hydrogen gas and oxidizers, Ar gas is still flowing through the system and the temperature is fixed to 0^oC so the system is left for cooling under Ar ambient.

4.2.1. Test Growth

The parameters used to test growths without oxidizing gases showed in Table 4.1. The optimal studied parameters of the system were determined with these studies. These parameters are then used for the presence of the oxidizing gas in the CNT growth. Many different parameters were tested without the oxidizing gas during CNT growth as shown Table 4.1. Magnifications in these parameters used for oxidizers as well.

Table 4.1. Parameters used in the optimization growth of CNTs without oxidizers (sccm= standart cm^3/min.).

Name of sample	Pressure (atm)	Tem. (^oC)	Ar (sccm)	H_2 (sccm)	C_2H_4 (sccm)	Growth time (min.)
FeAlO12CNT471	1	750	150	140	180	10
FeAlO11CNT472	1	750	150	140	180	10
FeAlO12CNT473	1	750	150	140	180	10
FeAlO11CNT474	1	750	150	140	180	10
FeAlO12CNT475	1	740	150	140	180	15
FeAlO11CNT476	1	740	150	140	180	15
FeAlO13CNT477	1	740	150	150	180	10
FeAlO12CNT478	1	740	150	150	180	10
FeAlO13CNT479	1	750	150	150	180	10
FeAlO12CNT480	1	750	150	150	180	10
FeAlO13CNT481	1	750	120	100	120	10
FeAlO13CNT482	1	750	120	100	120	10
FeAlO13CNT483	1	750	150	210	180	10
FeAlO11CNT484	1	750	150	210	180	10
FeAlO11CNT485	1	750	300	400	360	10
FeAlO11CNT486	1	750	300	400	360	10
FeAlO13CNT487	1	750	300	400	360	10
FeAlO13CNT488	1	750	225	225	270	10
FeAlO12CNT489	1	750	225	225	270	10
FeAlO11CNT490	1	750	225	225	270	10
FeAlO11CNT491	1	750	225	225	270	10
FeAlO12CNT492	1	750	75	100	90	10
FeAlO12CNT493	1	750	75	100	90	10
FeAlO12CNT494	1	750	75	100	90	10
FeAlO12CNT495	1	750	75	100	90	10
FeAlO12CNT496	1	750	75	100	90	10
FeAlO13CNT501	1	750	150	150	180	10
FeAlO13CNT502	1	750	150	150	180	10
FeAlO11CNT503	1	750	150	150	180	10
FeAlO11CNT504	1	750	150	150	180	10
FeAlO08CNT509	1	750	150	150	180	10
FeAlO08CNT510	1	750	150	150	180	10
FeAlO08CNT511	1	750	150	150	180	10
FeAlO13CNT514	1	740	300	400	360	15
FeAlO13CNT515	1	740	300	400	360	15
FeAlO13CNT516	1	740	300	400	360	15
FeAlO11CNT517	1	740	300	400	360	15
FeAlO11CNT519	1	740	300	500	360	15
FeAlO13CNT520	1	740	300	500	360	15
FeAlO11CNT521	1	740	300	500	360	15
FeAlO11CNT522	1	740	300	500	360	15

4.2.2. Growth with Oxidizers

In the experiments done in presence of CO_2, O_2 and H_2O, pretreatment time and oxidizer gas flows were main parameters studied (Table 4.2-Table 4.5). As well as these main parameters, we also varied growth temperature in presence of CO_2 as shown in Table 4.2.

Table 4.2. Studied parameters in the nanotube growth with the oxidizing gas CO_2 during growth time; Pressure: 1 atm., Ar: 150 sccm, H_2: 140 sccm

Sample name	T (^oC)	pretreatment		CNT growth		
		CO_2 (sccm)	Time (min.)	C_2H_4 (sccm)	CO_2 (sccm)	Time (min.)
FeAlO11CNT537	740	10	15	180	1	15
FeAlO11CNT538	740	10	15	180	1	15
FeAlO13CNT539	740	10	15	180	1	15
FeAlO11CNT540	740	10	10	180	1	15
FeAlO13CNT541	740	10	10	180	1	15
FeAlO11CNT542	740	10	10	180	1	15
FeAlO11CNT543	740	10	5	180	1	15
FeAlO11CNT544	740	10	5	180	1	15
FeAlO13CNT545	740	10	5	180	1	15
FeAlO11CNT546	740	10	2	180	1	15
FeAlO11CNT547	740	10	2	180	1	15
FeAlO11CNT548	740	10	2	180	1	15
FeAlO11CNT549	740	5	15	180	1	15
FeAlO11CNT550	740	5	15	180	1	15
FeAlO13CNT551	740	5	10	180	1	15
FeAlO11CNT552	740	5	10	180	1	15
FeAlO11CNT553	740	5	10	180	1	15
FeAlO11CNT554	740	5	5	180	1	15
FeAlO11CNT555	740	5	5	180	1	15
FeAlO11CNT556	740	5	5	180	1	15
FeAlO11CNT557	740	5	2	180	1	15
FeAlO11CNT558	740	5	2	180	1	15
FeAlO11CNT559	740	5	2	180	1	15
FeAlO11CNT560	740	10	15	180	2	15
FeAlO11CNT561	740	10	15	180	2	15
FeAlO13CNT562	740	10	15	180	2	15
FeAlO13CNT563	740	10	10	180	2	15

(cont. on next page)

Table 4.2 (cont.)

FeAlO13CNT564	740	10	10	180	2	15
FeAlO11CNT565	740	10	10	180	2	15
FeAlO11CNT566	740	10	10	180	2	15
FeAlO11CNT567	740	10	5	180	2	15
FeAlO11CNT568	740	10	5	180	2	15
FeAlO13CNT569	740	10	5	180	2	15
FeAlO11CNT570	740	10	2	180	2	15
FeAlO11CNT571	740	10	2	180	2	15
FeAlO13CNT572	740	10	2	180	2	15
FeAlO11CNT573	740	5	15	180	2	15
FeAlO11CNT574	740	5	15	180	2	15
FeAlO13CNT575	740	5	15	180	2	15
FeAlO13CNT576	740	5	10	180	2	15
FeAlO11CNT577	740	5	10	180	2	15
FeAlO11CNT578	740	5	10	180	2	15
FeAlO13CNT579	740	5	5	180	2	15
FeAlO11CNT580	740	5	5	180	2	15
FeAlO11CNT581	740	5	5	180	2	15
FeAlO13CNT582	740	5	2	180	2	15
FeAlO13CNT583	740	5	2	180	2	15
FeAlO11CNT584	740	5	2	180	2	15
FeAlO14CNT586	740	2	15	180	2	15
FeAlO14CNT587	740	2	15	180	2	15
FeAlO13CNT588	740	2	10	180	2	15
FeAlO14CNT589	740	2	10	180	2	15
FeAlO14CNT590	740	2	10	180	2	15
FeAlO14CNT591	740	2	5	180	2	15
FeAlO14CNT592	740	2	5	180	2	15
FeAlO14CNT593	740	2	2	180	2	15
FeAlO14CNT594	740	2	2	180	2	15
FeAlO14CNT595	740	2	15	180	1	15
FeAlO14CNT596	740	2	15	180	1	15
FeAlO14CNT597	740	2	10	180	1	15
FeAlO14CNT598	740	2	10	180	1	15
FeAlO14CNT599	740	2	5	180	1	15
FeAlO14CNT600	740	2	5	180	1	15
FeAlO14CNT603	740	2	2	180	1	15
FeAlO14CNT611	760	10	15	180	2	15
FeAlO14CNT612	760	10	10	180	2	15
FeAlO14CNT613	760	10	5	180	2	15
FeAlO14CNT614	760	10	2	180	2	15
FeAlO14CNT616	760	10	15	180	1	15

(cont. on next page)

Table 4.2 (cont.)

FeAlO14CNT617	760	10	10	180	1	15
FeAlO14CNT618	760	10	5	180	1	15
FeAlO14CNT619	760	10	2	180	1	15
FeAlO14CNT620	760	5	15	180	2	15
FeAlO14CNT621	760	5	10	180	2	15
FeAlO14CNT630	760	5	15	180	1	15
FeAlO14CNT631	760	5	10	180	1	15
FeAlO14CNT632	760	5	5	180	1	15
FeAlO14CNT637	760	5	2	180	1	15
FeAlO14CNT638	760	2	15	180	2	15
FeAlO14CNT639	760	2	10	180	2	15
FeAlO14CNT640	760	2	5	180	2	15
FeAlO14CNT641	760	2	2	180	2	15
FeAlO14CNT642	760	2	15	180	1	15
FeAlO14CNT643	760	2	10	180	1	15
FeAlO14CNT644	760	2	5	180	1	15
FeAlO14CNT646	760	2	2	180	1	15

Table 4.3. Studied parameters in the nanotube growth with different pretreatment times in the presence of CO_2 (P: 1 atm., T: 760 ^oC, Ar: 150 sccm during growth)

Name of sample	Pretreatment				CNT growth		
	H_2		CO_2		C_2H_4 (sccm)	CO_2 (sccm)	Time (min.)
	amont (sccm)	time min.	amount(sccm)	time (min)			
FeAlO14CNT647	140	10	10	5	180	2	15
FeAlO14CNT648	140	5	10	10	180	1	15
FeAlO14CNT649	140	13	10	2	180	1	15
FeAlO14CNT650	140	13	5	2	180	2	15
FeAlO14CNT651	140	10	5	5	180	1	15
FeAlO14CNT652	140	13	2	2	180	2	15
FeAlO14CNT653	140	5	10	5	180	2	15
FeAlO14CNT654	140	5	5	5	180	2	15
FeAlO14CNT655	140	5	2	5	180	1	15
FeAlO14CNT656	140	3	5	2	180	1	15

Table 4.4. Studied parameters in the nanotube growth with the oxidizer gas O_2 and different pretreatment times; P: 1 atm., T: 760 ^oC, Ar: 150 sccm H_2: 140 sccm.

Name of sample	Pretreatment		CNT Growth		
	O_2 (sccm)	time (min.)	C_2H_4 (sccm)	O_2 (sccm)	time (min.)
FeAlO14CNT657	5	15	180	2	15
FeAlO14CNT658	5	10	180	2	15
FeAlO14CNT659	5	5	180	2	15
FeAlO14CNT660	5	2	180	2	15
FeAlO14CNT661	5	15	180	1	15
CoAlO2CNT662	5	15	180	1	15
FeAlO14CNT663	5	10	180	1	15
CoAlO1CNT664	5	10	180	1	15
CoAlO2CNT665	5	10	180	1	15
FeAlO14CNT666	5	5	180	1	15
CoAlO1CNT667	5	5	180	1	15
CoAlO2CNT668	5	5	180	1	15
FeAlO14CNT669	5	2	180	1	15
CoAlO1CNT670	5	2	180	1	15
CoAlO2CNT671	5	2	180	1	15
CoAlO1CNT672	2	15	180	2	15
CoAlO2CNT673	2	15	180	2	15
FeAlO14CNT674	2	15	180	2	15
FeAlO14CNT675	2	10	180	2	15
CoAlO1CNT676	2	10	180	2	15
CoAlO2CNT677	2	10	180	2	15
FeAlO14CNT678	2	10	180	2	15
CoAlO1CNT679	2	10	180	2	15
CoAlO2CNT680	2	10	180	2	15
FeAlO14CNT681	2	15	180	0.5	15
CoAlO1CNT682	2	15	180	0.5	15
CoAlO2CNT683	2	15	180	0.5	15
FeAlO14CNT684	2	5	180	0.5	15
CoAlO1CNT685	2	5	180	0.5	15
CoAlO2CNT686	2	5	180	0.5	15
FeAlO14CNT687	0.5	15	180	-	15
CoAlO1CNT688	0.5	15	180	-	15
CoAlO2CNT689	0.5	15	180	-	15
FeAlO14CNT690	-	15	180	-	15
CoAlO1CNT691	-	15	180	-	15
CoAlO2CNT692	-	15	180	-	15

Table 4.5. Studied parameters in the nanotube growth with the oxidizer gas H_2O and different pretreatment times; P: 1 atm., T: 760 ^oC, Ar: 150 sccm H_2: 140 sccm.

Name of sample	Pretreatment		CNT growth		
	H_2O (^oC) (Tip)	time (min.)	C_2H_4 (sccm)	H_2O (^oC) (Tip)	time (min.)
FeAlO14CNT693	60(A)	15	180	60(A)	15
CoAlO1CNT694	60(A)	15	180	60(A)	15
CoAlO2CNT695	60(A)	15	180	60(A)	15
FeAlO14CNT696	60(A)	15	180	60(B)	15
CoAlO1CNT697	60(A)	15	180	60(B)	15
CoAlO2CNT698	60(A)	15	180	60(B)	15
FeAlO14CNT699	60(B)	15	180	60(A)	15
FeAlO14CNT700	60(B)	15	180	60(B)	15
FeAlO14CNT701	50(A)	15	180	50(A)	15
FeAlO14CNT702	50(A)	15	180	50(B)	15
FeAlO14CNT703	70(A)	15	180	70(A)	15
FeAlO14CNT704	70(A)	15	180	70(B)	15
FeAlO14CNT706	70(B)	15	180	70(A)	15
FeAlO14CNT707	70(B)	15	180	70(B)	15
FeAlO14CNT709	60(A)	15	180	70(A)	15
FeAlO14CNT710	60(A)	15	180	70(B)	15
FeAlO14CNT711	70(A)	15	180	70(A)	15
FeAlO14CNT712	70(A)	15	180	70(B)	15
FeAlO14CNT713	60(A)	15	180	60A)	15
FeAlO04CNT714	60(A)	15	180	60(A)	15
FeAlO05CNT715	60(A)	15	180	60(A)	15
FeAlO06CNT716	60(A)	15	180	60(A)	15
FeAlO07CNT717	60(A)	15	180	60(A)	15
FeAlO09CNT718	60(A)	15	180	60(A)	15
FeAlO10CNT719	60(A)	15	180	60(A)	15
FeAlO12CNT720	60(A)	15	180	60(A)	15
FeAlO14CNT721	60(A)	15	180	60(A)	15
FeAlO14CNT722	60(A)	15	180	60(A)	15
FeAlO14CNT723	60(A)	15	180	60(A)	15
FeAlO10CNT724	60(A)	15	180	60(A)	15
FeAlO12CNT725	60(A)	15	180	60(A)	15
FeAlO14CNT730	60(A)	15	180	60(A)	15
FeAlO12CNT731	60(A)	15	180	60(A)	15
FeAlO14CNT732	60(A)	15	180	60(B)	15
FeAlO12CNT733	60(A)	15	180	60(B)	15
FeAlO12CNT734	70(A)	15	180	70(A)	15
FeAlO14CNT735	70(A)	15	180	70(A)	15
FeAlO12CNT736	70(B)	15	180	70(B)	15
FeAlO09CNT737	70(B)	15	180	70(B)	15
FeAlO14CNT738	70(B)	15	180	70(B)	15

4.3. Characterization Techniques

Characterization is the most significant part to discuss the results and the characterization techniques used for examining the samples give absolutely significant properties about the samples. This study is a parametric research in order to find optimal growth and pretreatment conditions for high quality and high yield so characterization of obtained CNTs is essential. In this study, SEM (Scanning Electron Microcopy) and Raman Spectroscopy were used.

4.3.1. Scanning Electron Microscopy

SEM (Scanning Electron Microscopy) is the most important method to analyze carbon nanotube growths. Morphology of CNTs, their dimensions, their densities and their growth orientations can be readily seen by SEM (Thess, et al. 1996; Liu, et al. 2004; Li, et al. 2002). SEM is utilized to measure the diameter of CNTs and to observe the density of CNTs on the surface during this study.

Electron beams, thermionically emitted from an electron gun is send on the specimen surface, several signals can be detected. By sending the primary electron, high energy backscattered electrons appear and primary electron can be diffracted with large angles. When these backscattered electrons emerge from the surface, secondary electrons are generated. Electron beams have energies ranging from a few thousand eV to 50 keV. Pairs of scanning coils located at the objective lens deflect the beam either linearly.

4.3.2. Raman Spectroscopy

Raman spectroscopy is generally used to study the structural quality of CNTs. This technique can be used to the details about the CNTs configuration. This tool also gives information about the number of walls, the presence of crystalline, amorphous carbon and yield diameters of SWCNTs.

The basic principle of Raman Spectroscopy is that a beam of light sent onto a sample emerges scattered in different directions than the incoming beam. Most of this

scattered light is of unchanged wavelength, but a small part has wavelengths different from the incident light, and its presence is a result of Raman effect. Micro-Raman spectroscopy is used for characterization of CNTs with a 633 nm, 514.5 nm and 488 nm wavelength lasers.

The characteristic spectrum of SWNTs exhibits three main zone; low (100-250 cm^{-1}), intermediate (300-1300 cm^{-1}) and high (1500-1600cm^{-1}) frequencies (Journet, et al. 1997; Colomer, et al 2000). These three zones have also other names, as Radial Breathing Modes (RBM), D (disordered)- modes, and G (graphite)-modes, respectively.

The radial breathing mode is located around 191 and 216 cm^{-1} at low energy peaks in CNTs (Rao, et al. 1997), and can be clearly observed using He-Ne laser (Lee, et al. 1997). The RBM is of crucial important since it gives valuable information about the diameter distribution of SWNTs. This mode is very sensitive to the diameter of SWNTs and generally seen for CNT diameters of up to 3 nm.

The D peak is located around 1300 cm^{-1} when He-Ne laser, or at 1350 cm^{-1} when Ar ion laser used as excitation source. The D peak indicates the presence of structural defects (Geng, et al. 2002). The other important peak is the G peak and it is located around 1580 cm^{-1}, which is associated with the in-plane vibrations of the graphene sheet (Singh, et al. 2003; Shanov, et al. 2006). The G mode can be decomposed in one main peak with a shoulder (Rao, et al. 1997; Dresselhaus, et al. 2002). That is this band have two different components, the lower frequency component associated with vibrations along the circumferential direction, (G_-), and the higher frequency component, (G_+), attributed to vibrations along the direction of the nanotube axis. These peaks give information about the CNTs; whether they are semiconducting or metallic (Rotkin and Subramoney 2005; Reich, et al. 2004).

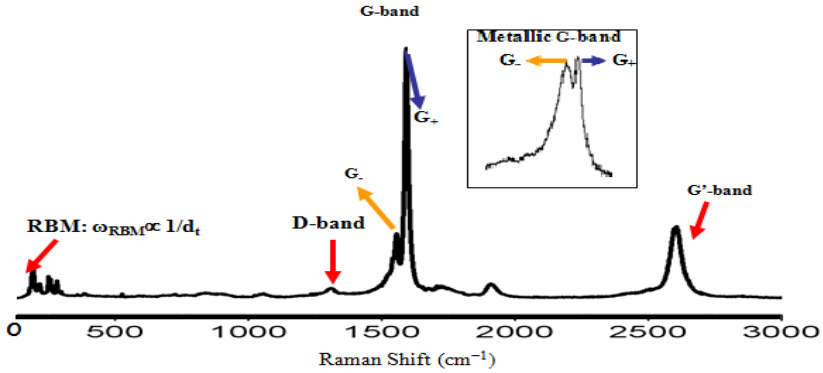

Figure 4.3. Raman spectra showing the main peaks and the characters of SWNTs (Source: Dresselhaus, et al. 2002)

CHAPTER 5

RESULTS AND DISCUSSION

First section in this chapter focuses on determining the optimal growth parameters without aid of oxidizers. SEM images were used to calculate diameters of CNTs. Then, we carried out experiments to observe the effects of weak oxidizers (CO_2, H_2O, O_2) on CNT diameters. In presecence of CO_2, several pretreatment and growth parameters were studied. In this section, firstly, the results of CO_2 gas flow rates and pretreatment atmosphere (to obtain high quality CNT) are discussed. After determining best pretreatment and gas flow rates; in the following section the effect of temperature on the CNT growth is examined. In the second section, the effects of O_2 on effective CNT growth are investigated. Pretreatment time and gas flow rates are examined in the presence of O_2. In the third section, the effects of H_2O are analyzed by using SEM images, and parameters adjusted accordingly in order to obtain high quality CNT. At the last part, all data were subjected to through extensive statistical analysis. To draw conclusion, SEM and Raman spectroscopy characterization analysis results were used.

5.1. SEM Results

5.1.1. The Optimal Growth Parameters without Oxidizers

Optimal growth parameters were determined according to SEM results. From the structural quality of CNTs Ar: 150 sccm, H_2: 140 sccm, C_2H_4: 180 sccm, temperature: 740 ^oC, growth time: 15 minutes were closer as optimal parameters. The SEM images (Figure 5.1) of the as-grown samples were used to obtain the average diameters and related diameter distributions (Figure 5.2).

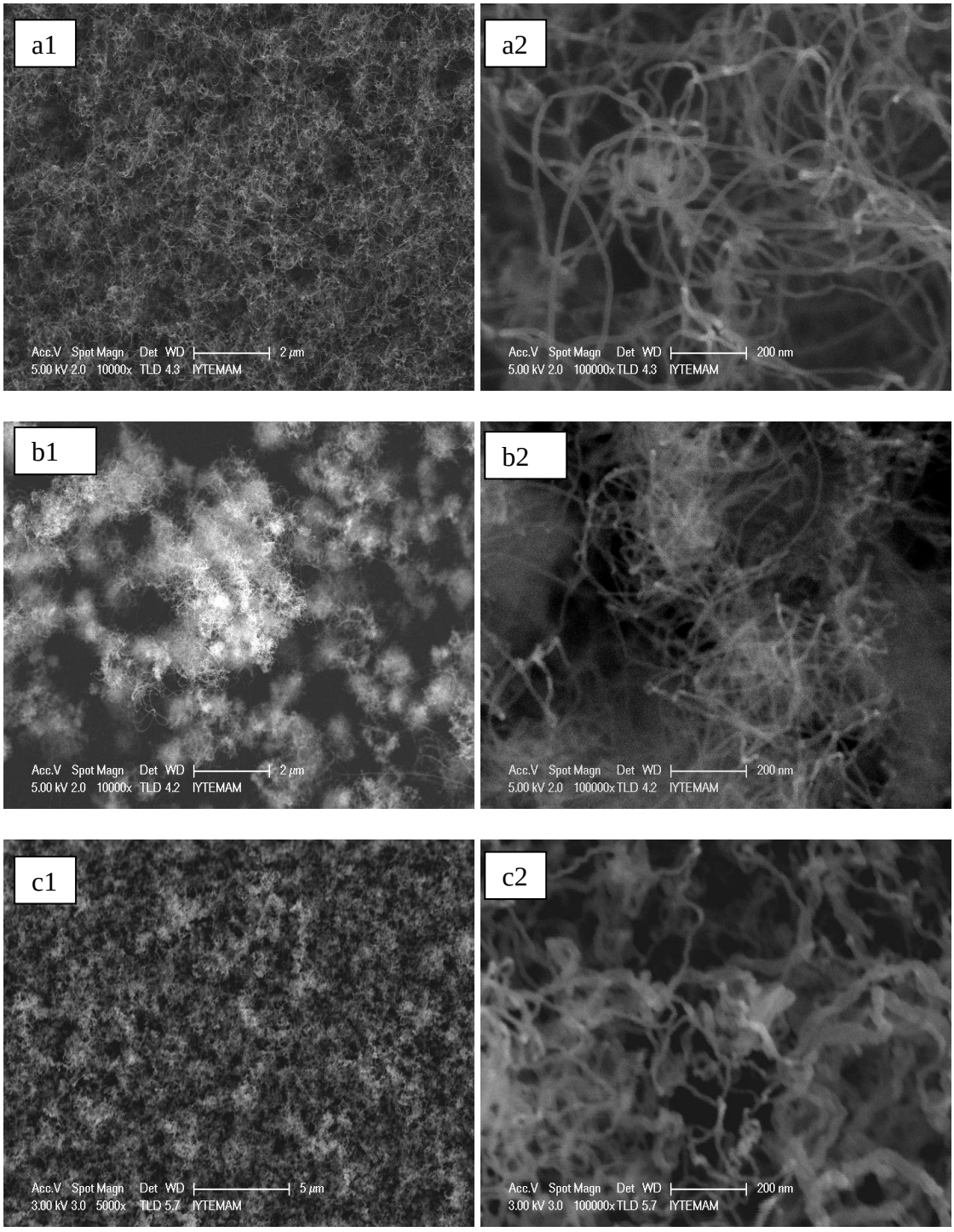

Figure 5.1. SEM images of CNTs a) FeAlO11CNT476 b) FeAlO11 CNT485 c) FeAlO11 CNT472 d) FeAlO11 CNT484 e) FeAlO11 CNT486 f) FeAlO11 CNT517; Magnification; 1= 10 000x (a and b); 1=5 000x (c, d, e, f) ; 2= 100 000x

(cont. on next page)

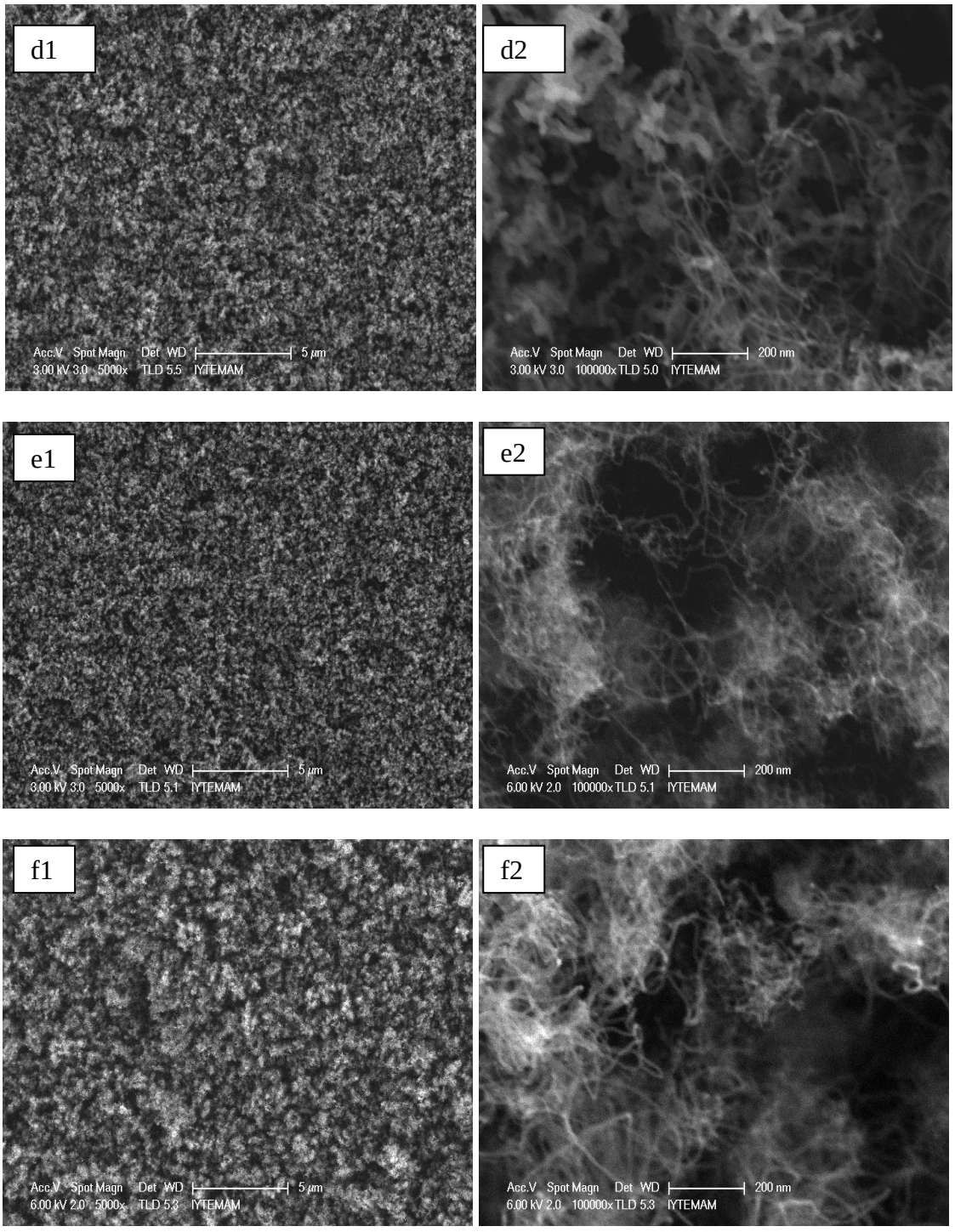

Figure 5.1. (cont.)

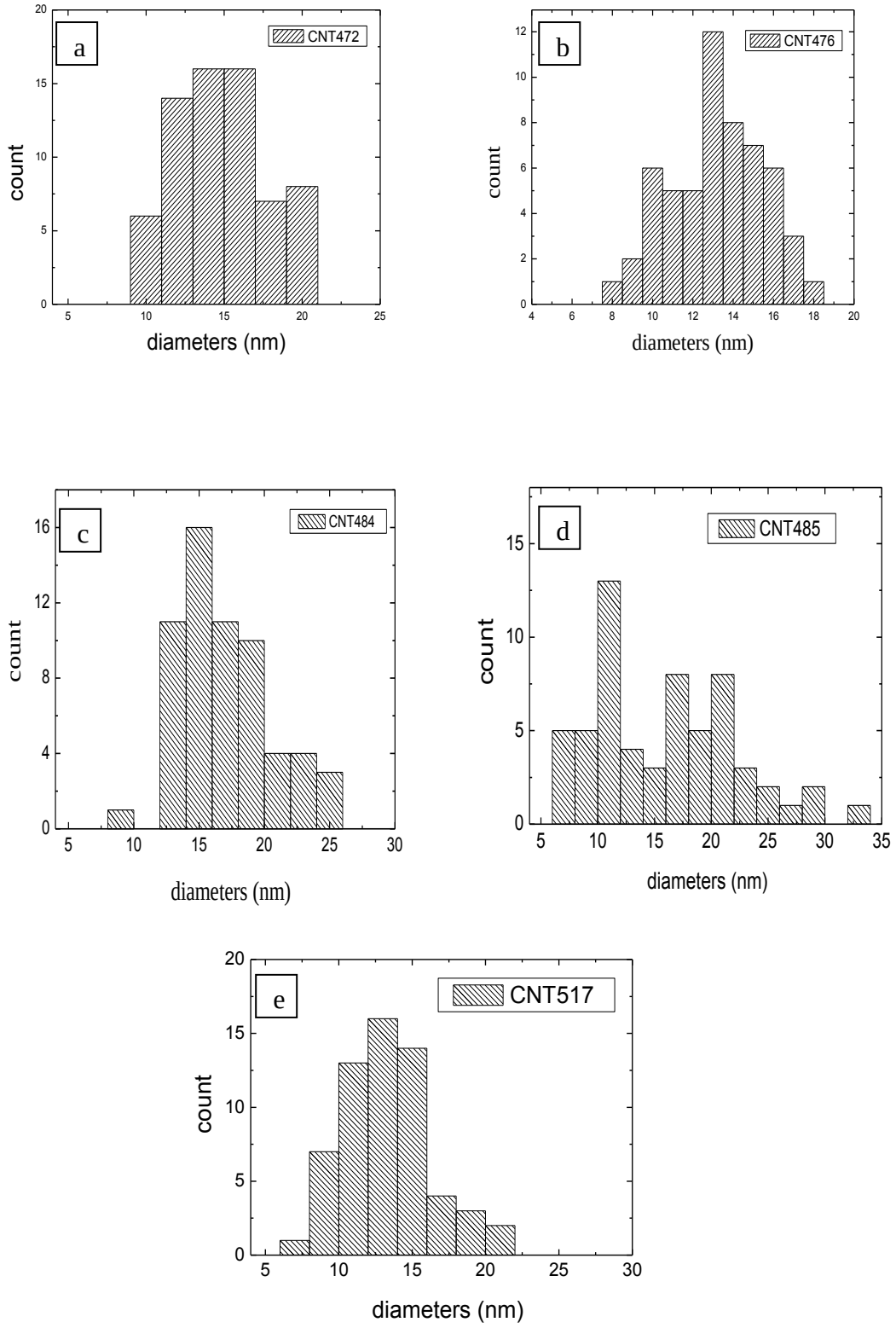

Figure 5.2. Diameter distributions of CNTs without oxidizers a) FeAlO11 CNT472, b) FeAlO11 CNT476, c) FeAlO11 CNT484, d) FeAlO11 CNT485, e) FeAlO11 CNT517.

5.1.2. The Role of CO_2 for Effective CNT Growth

Effects of adding CO_2 in pretreatment and growth stages were investigated on a variety of growth conditions in order to control CNT diameters. The main growth parameters studied in this part were CO_2 level, pretreatment time and temperature. Ethylene was used as the carbon source for CNT growth, while CO_2 was utilized as a catalyst enhancer and preserver. In the following discussion, we concentrate on how diameters of CNTs varied with the amount of CO_2 at a fixed growth temperature. A simple schedule was first set to grow CNTs in both CO_2 and hydrogen environment. CNT diameter distribution was obtained based on SEM images by measuring more than 70 tube diameters.

5.1.2.1. Pretreatment Effect

The role of CO_2 in the CNT growth with TCVD technique by ethylene decomposition was investigated by changing both pretreatment duration and CO_2 level using the thin Fe film sputtered on two SiO_2/Si substrates (FeAlO11; FeAlO13). Smaller amount CO_2 was continued to send during growth time in this part. Here, we studied pretreatment times of 15, 10, 5, 2 minutes. In addition, CO_2 at a flow rates, 10:1, 10:2, 5:1, 5:2, 2:1 and 2:2 sccm, were send in system during both pretreatment and growth stages. CNT SEM images were characterized in order to see effects of CO_2 under growth conditions. It was observed that the catalyst particle sizes were increased with increased pretreatment time at the gas flows of 10:1 and 5:1 pretreatment/growth ratios. This condition had a change of the reducing of metal-oxide to metal film with H_2 and controlling of the reduction rate of metal-oxide film with CO_2. Formed catalyst particles are mobile and can form larger clusters with the effect of high temperature when they are in the elemental form and they occur very fast especially on SiO_2 layer. Large nanoparticles are not very effective for CNT growth, and at the same time decrease the density of CNTs per unit area. H_2 and CO_2 amounts play significant role in this process. According to our results, the optimal particle sizes were obtained by calibrating both pretreatment time and CO_2 level. The mean diameters are given in the Table 5.1.

Table 5.1. The amounts of CO_2 used during various pretreatment and growth times and the mean diameters obtained as a result.

Sample	Temperature (^{0}C)	Pretreatment time (min.)	CO_2(p)/CO_2(g) (sccm)	The mean diameters (nm)
FeAlO11CNT537	740	15	10/1	12.5
FeAlO11CNT542	740	10	10/1	10.0
FeAlO13CNT545	740	5	10/1	9.5
FeAlO11CNT548	740	2	10/1	8.8
FeAlO11CNT561	740	15	10/2	6.1
FeAlO11CNT566	740	10	10/2	6.7
FeAlO13CNT569	740	5	10/2	6.8
FeAlO13CNT572	740	2	10/2	11.2
FeAlO11CNT549	740	15	5/1	9.8
FeAlO11CNT552	740	10	5/1	9.3
FeAlO11CNT554	740	5	5/1	8.9
FeAlO11CNT559	740	2	5/1	6.1
FeAlO11CNT574	740	15	5/2	5.7
FeAlO11CNT578	740	10	5/2	6.3
FeAlO11CNT581	740	5	5/2	7.3
FeAlO11CNT584	740	2	5/2	7.3

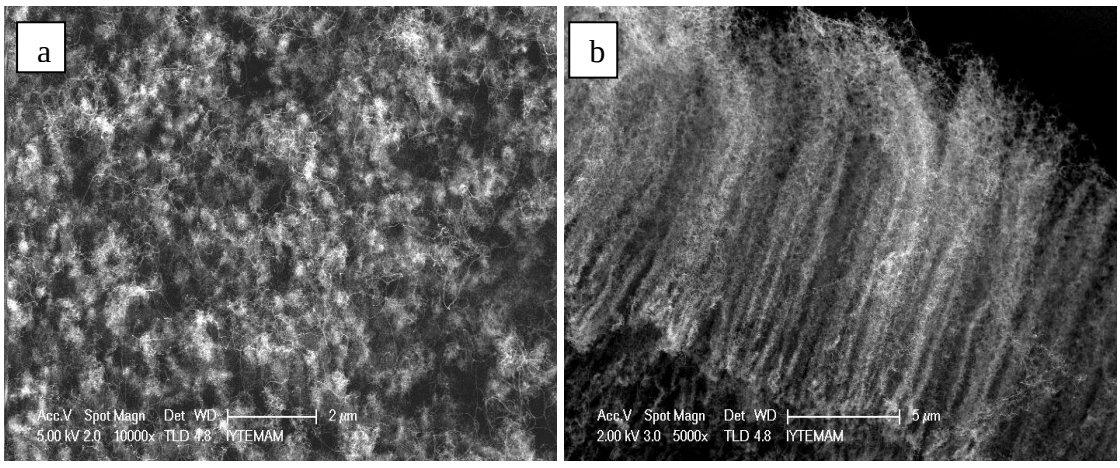

Figure 5.3. The growth with CO_2 at 740°C a), b) FeAlO11 CNT537 15 min., c), d) FeAlO12 CNT542 10 min., e), f) FeAlO13CNT545 5 min., g), h) FeAlO11 CNT548 2min.

(cont. on next page)

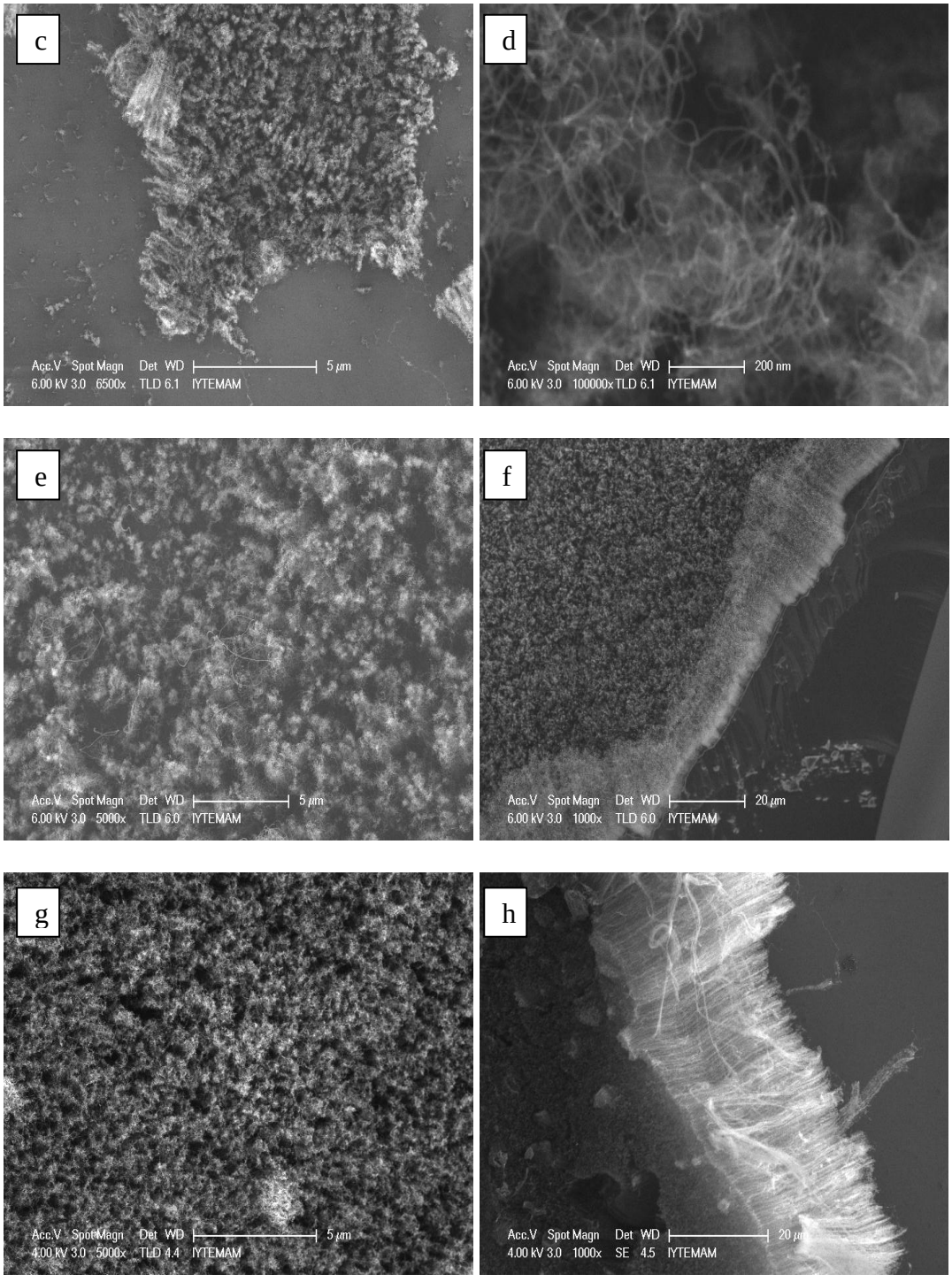

Figure 5.3. (cont.)

Once we carefully examined SEM results, we have seen that the CNT growths which were exposed shorter pretreatment time had smaller mean diameters, and narrower diameter distributions were densely packed. Sides and angled views showed that samples grown in 15 and 10 min. were less densely populated those grown in 5 and 2 minutes (Figure 5.3). This decreased density of CNTs can be explained by catalyst

particles' forming bigger particles. When we measured CNT diameters, we observed that the range was between 5 nm and 8 nm at short pretreatment time as shown in Figure 5.4.

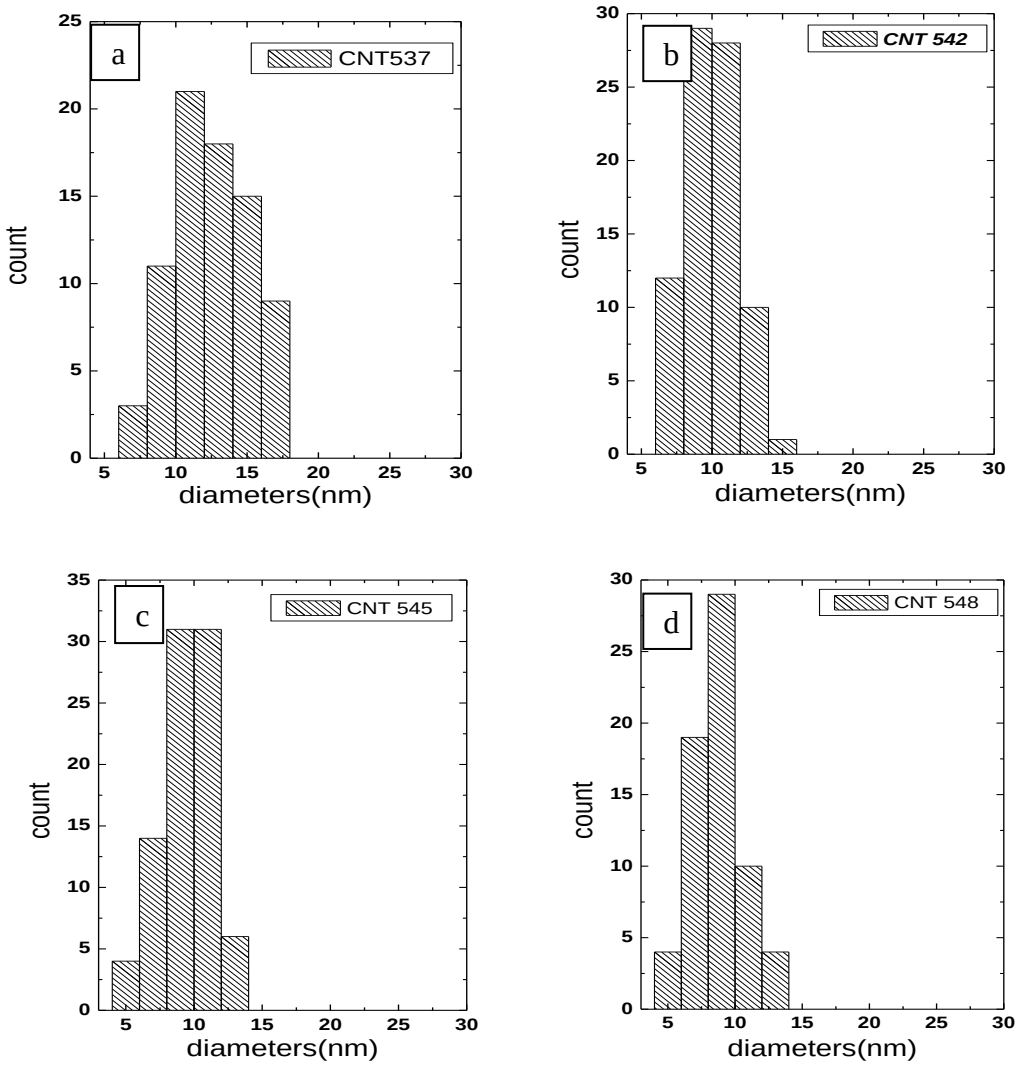

Figure 5.4. The analyses of the catalyst particle sizes occured by pretreatment time a) 15 min., b) 10 min., c) 5 min., d) 2 min.

We, in detail, analyzed how mean diameters depended on pretreatment timing as shown in Figure5.5. In presence of CO_2 during pretreatment process, high concentration (10 sccm) of CO_2 and short pretreatment time caused CNTs to had larger diameters irrespective of CO_2 amount in growth stage. When pretreatment time is increased to higher amounts of CO_2, diameters of CNTs obtained with 2 sccm CO_2 at growth stage were immediately observed to be decreasing but at growth stage, diameters of CNTs

obtained with 1 sccm CO_2 was increasing. A reason for this can be explained: In the presence of high CO_2, reduction of metal-oxide to metal is not totally carried out, thus resulting in large nanoparticles and associated CNT diameters are large. The cause of immediate decrease in diameters with pretreatment time the samples at high CO_2 during pretreatment stage and 2 sccm CO_2 during growth prevented that sufficient oxygen did not allow growth of smaller catalyst particles in growth stage with the effects of both temperature and higher hydrogen amount.

2 sccm CO_2 amount used during growth time resulted in smaller diameters than 1 sccm CO_2 amount used during growth time as shown in Figure 5.5.

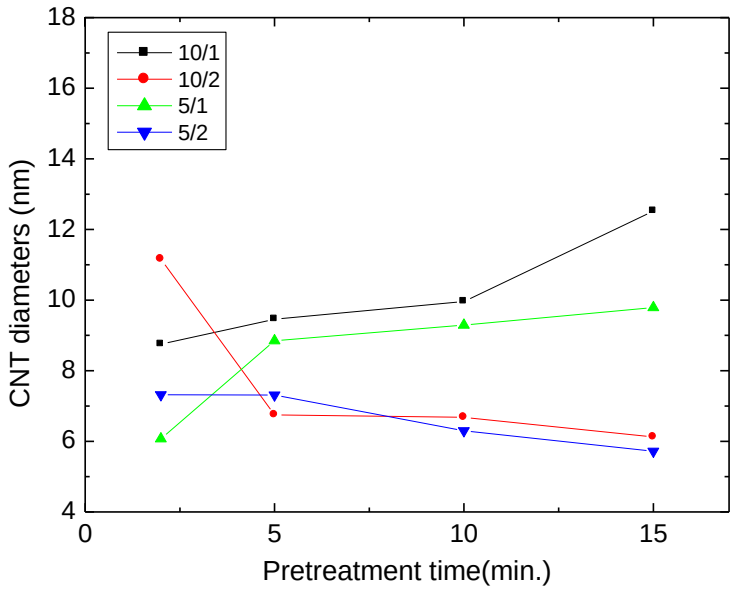

Figure 5.5. Depence of mean diameters on pretreatment duration and CO_2 amount

5.1.2.2. Temperature Effect

We carried out experiments to study the influence of temperature in CO_2-assisted CVD. Four different pretreatment times were studied at two different growth temperatures. We investigated the effect of CO_2 (2sccm) at different growth temperatures on the thin Fe films sputtered on $Al_2O_3/SiO_2/Si$. The mean diameters were ranging from 15 nm to 21 nm at 740 ^oC, however CNT diameters were changing between 5 nm and 8 nm at 760 ^oC as shown in Table 5.2.

Table 5.2. The variations of CNT diameters at different temperature

Sample	Temperature (^oC)	Pretreatment time (min.)	CO_2/H_2 (sccm)	Mean diameters (nm)
FeAlO14 CNT587	740	15	2/140	20.74
FeAlO14 CNT590	740	10	2/140	18.57
FeAlO14 CNT592	740	5	2/140	17.36
FeAlO14 CNT594	740	2	2/140	21.91
FeAlO14 CNT638	760	15	2/140	6.77
FeAlO14 CNT639	760	10	2/140	5.72
FeAlO14 CNT640	760	5	2/140	5.12
FeAlO14 CNT641	760	2	2/140	6.10

It was estimated that carbon reacted with oxygen to form CO owing to metal-oxide form of catalyst particle. If catalyst particle was kept at long enough pretreatment time and growth parameters were not suitable for growth, amorphous carbon coating on the catalyst surface instead of CNT growth occurs. If coming gas amount was very high or not mixed with suitable amount of H_2, all surfaces of substrate could be coated with carbon. This crude sceranio is greatly used in CNT growth, although what experimental conditions in the atomic dimensions happen is unknown in real.

It is known that catalyst film coalesces to form nanoparticles with effect of temperature and hydrogen and these particles uniformly spread over the whole surface. To obtain on effective growth it is necessary that the particles size have small size uniformly and narrowly distributed. It is expected that particles uniformly covers the whole surface and coalesce easily from film with help of temperature and hydrogen. The temperature plays very important role in this event. The coalescence happens after metal-oxide film converts to metal film. During pretreatment, CO_2 controls coalescence by controlling speed of metal oxide to metal translation. Also, CO_2 assists the growth process by removing amorphous carbon that forms throughout growth process. Experimental results show that diameters of CNTs were decreasing while the temperature was increasing. The cause of this was more effective reduction of metal-

oxide to metal form with increased temperature. At this state from film to particle conversion is easier.

By utilizing hydrogen and CO_2, we obtained both more dense CNTs and smaller diameters CNTs at higher temperature when we compared two different temperatures (Figure 5.6). These two temperatures were seen to have similar behavior with pretreatment time. Therefore, as well as CO_2, temperature was a significant parameter in order to determine diameters as the distributions are shown in Figure 5.7.

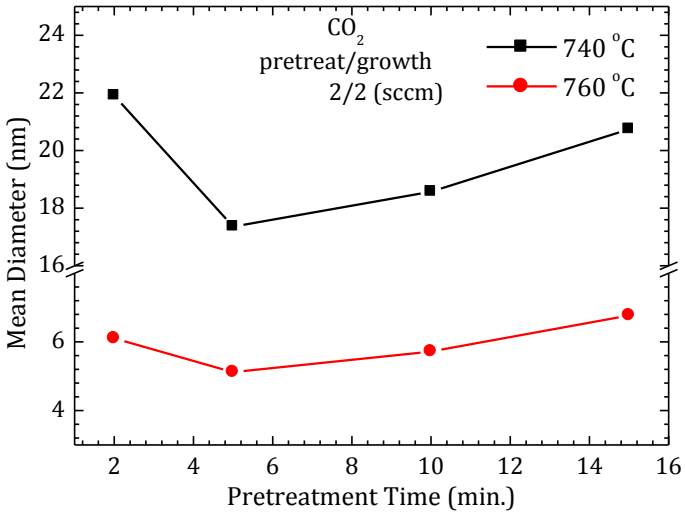

Figure 5.6. The variation of mean diameters of CNTs as function temperature

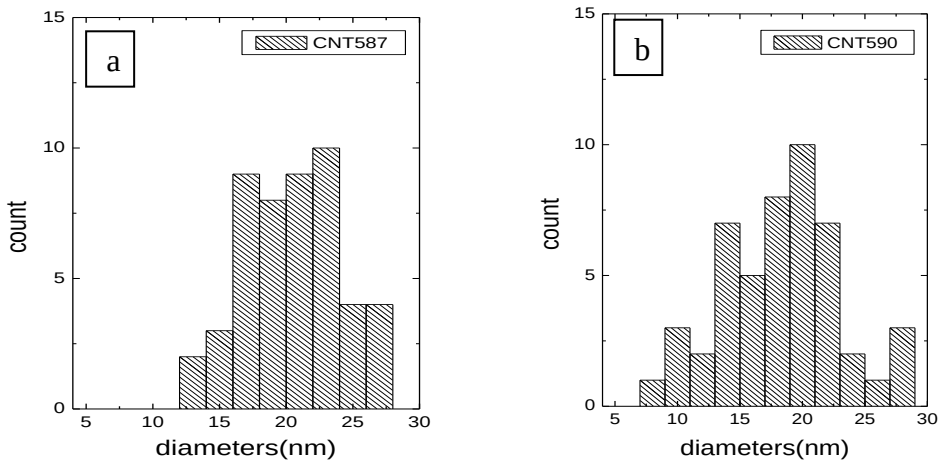

Figure 5.7. The diameter distributions of CNTs at different temperatures: a) 740 °C, 15 min. b) 740 °C , 10 min. c)740 °C, 5 min. d) 740 °C, 2 min. e)760 °C, 15 min. f)760 °C, 10 min. g) 760 °C, 5 min. h) 760 °C, 2 min.

(cont. on next page)

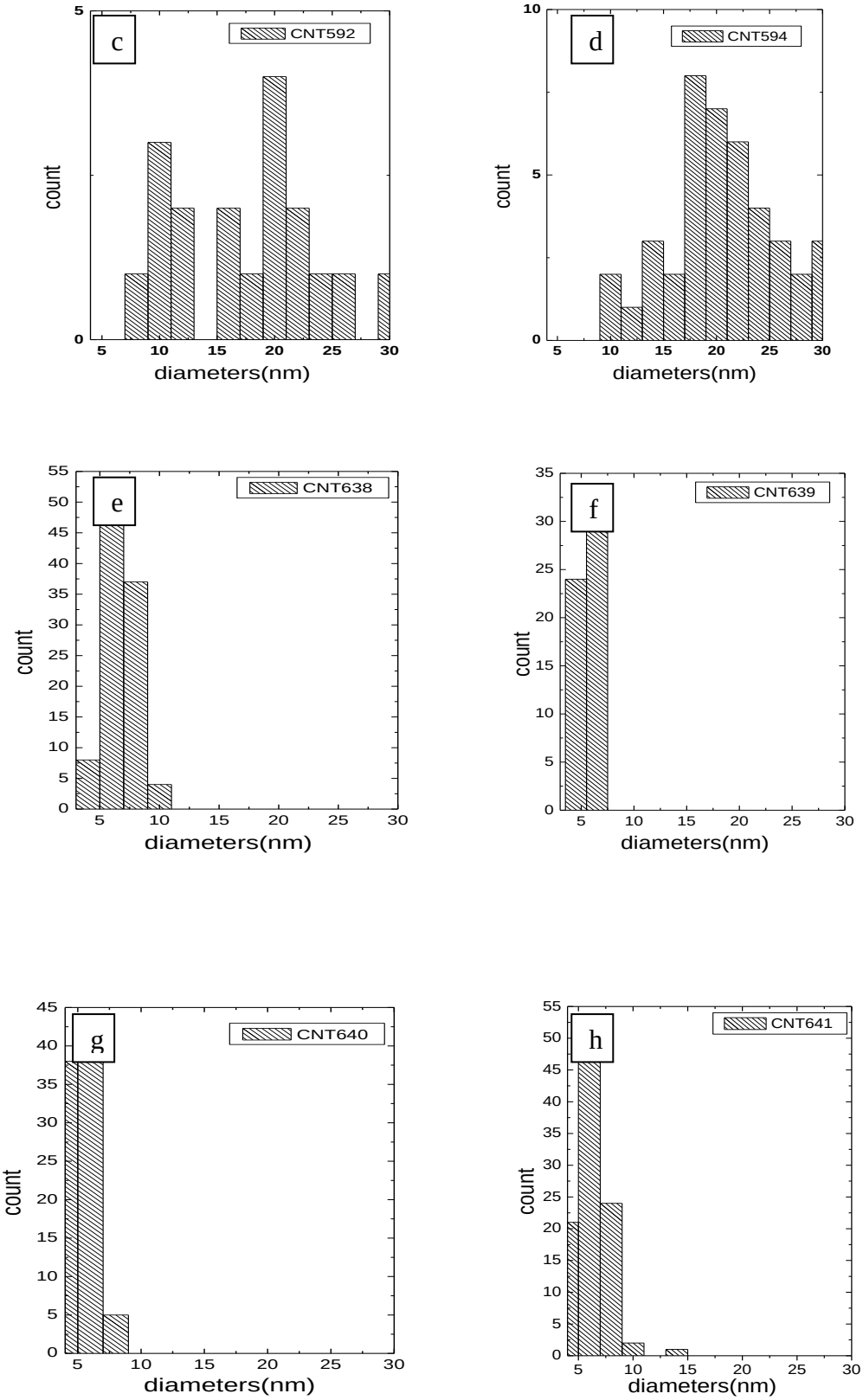

Figure 5.7. (cont.)

According to SEM analysis results (Figure 5.8), number of CNTs per unit area on the surface was low and diameters were changing between 15 nm and 20 nm at 740 ^{o}C. However, when we increased temperature to 760 ^{o}C, when we observed that both growth enhancement on the surface increased and diameters decreased. The diameters were between 5 nm and 6 nm.

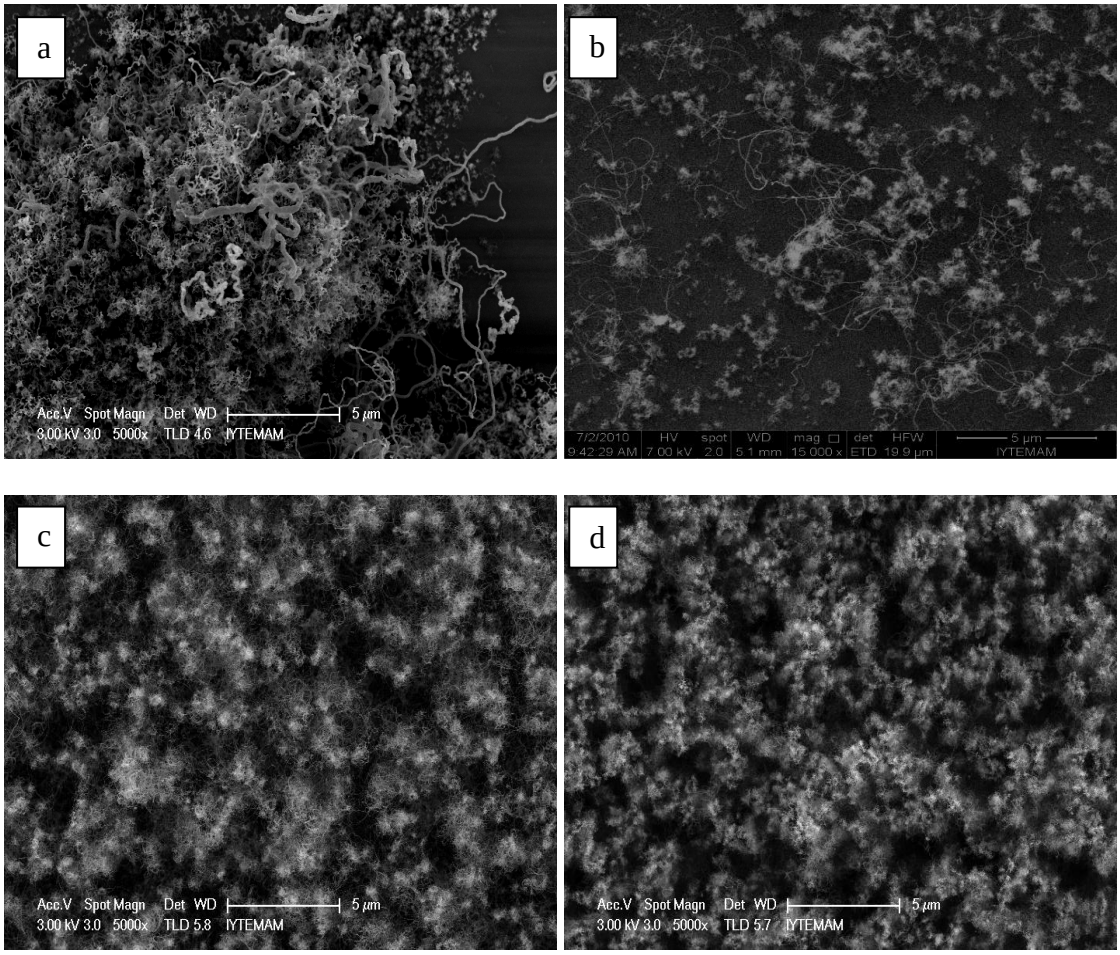

Figure 5.8. The growths with CO_2 at 740 °C ve 760 °C a) 740°C, FeAlO14 CNT587, 15 min. b) 740 °C, FeAlO14 CNT590, 10 min. c) 760°C, FeAlO14 CNT638, 15 min. d) 760 °C, FeAlO14 CNT640, 5 min.

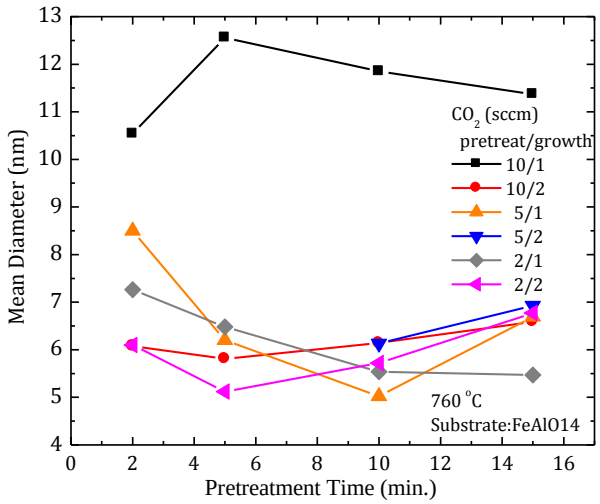

Figure 5.9. Dependence on CO_2 amount and pretreatment time at 760 °C of the mean diameters

It is seen in Figure 5.9 and in Figure 5.10 how obtained diameters from the growths made at 760°C depend on pretreatment time and pretreatment type. From these results it was possible to reduce the similar results with the samples grown at 740 °C. Except for pretreatment time of 10:1 sccm the diameters was decreasing once pretreatment time was increased, and then it was slowly increased. The diameters for both short pretreatment time and CO_2 level of 1 sccm were large. At large parts of 1 sccm oxidizer, this determined that the clustering of catalyst particle due to high temperature which lead to larger catalyst particles.

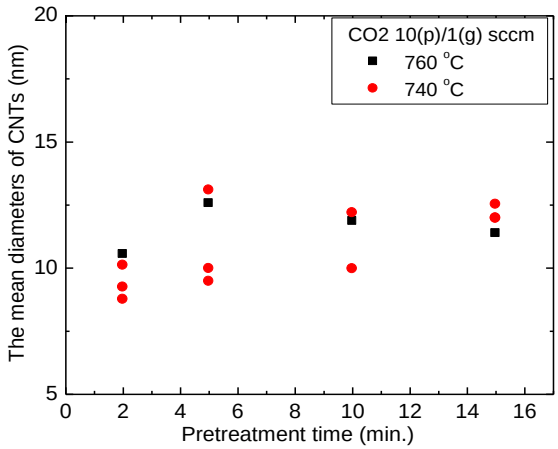

Figure 5.10. The variation of diameters with temperature the samples sending CO_2 of 10 sccm during pretreatment time and CO_2 of 1 sccm during growth time

5.1.2.3. Discontinuous Pretreatment Effect

The influence of CO_2 on CNT growth was also investigated by sending CO_2 later than H_2 in pretreatment. CO_2 flow rates were 10:1, 10:2, 5:2, 5:1, 2:2 and 2:1 sccm and pretreatment time with H_2 was 15 and 10 minutes, CO_2 send for 5 and 2 minutes (Table 5.3). Diameters were observed to change between 5 nm and 8 nm. Shorter pretreatment time of CO_2 compare to H_2 led to narrow diameter ranges (Table 5.3).

Table 5.3. CO_2 + H_2 gases in the different pretreatment time and the variations of diameters of CNTs

Sample	Temperature (^oC)	Pretreatment (min) H_2/CO_2	$CO_2(p)/CO_2(g)$ (sccm)	Mean diameters (nm)
FeAlO14CNT647	760	15/5	10/2	5.96
FeAlO14CNT648	760	15/10	10/1	8.07
FeAlO14CNT649	760	15/2	10/1	6.60
FeAlO14CNT650	760	15/2	5/2	7.02
FeAlO14CNT651	760	15/5	5/1	7.50
FeAlO14CNT652	760	15/2	2/2	5.45
FeAlO14CNT653	760	10/5	10/2	6.82
FeAlO14CNT654	760	10/5	5/2	4.69
FeAlO14CNT655	760	10/5	2/1	7.29
FeAlO14CNT656	760	5/2	5/1	8.90

When we analyzed SEM images, shorter pretreatment time of CO_2 compare to H_2, led to narrower range of the diameters as shown in Figure 5.11. Density of CNTs on the surface was larger dense and diameters change between 5 nm and 8 nm at 760 ^oC.

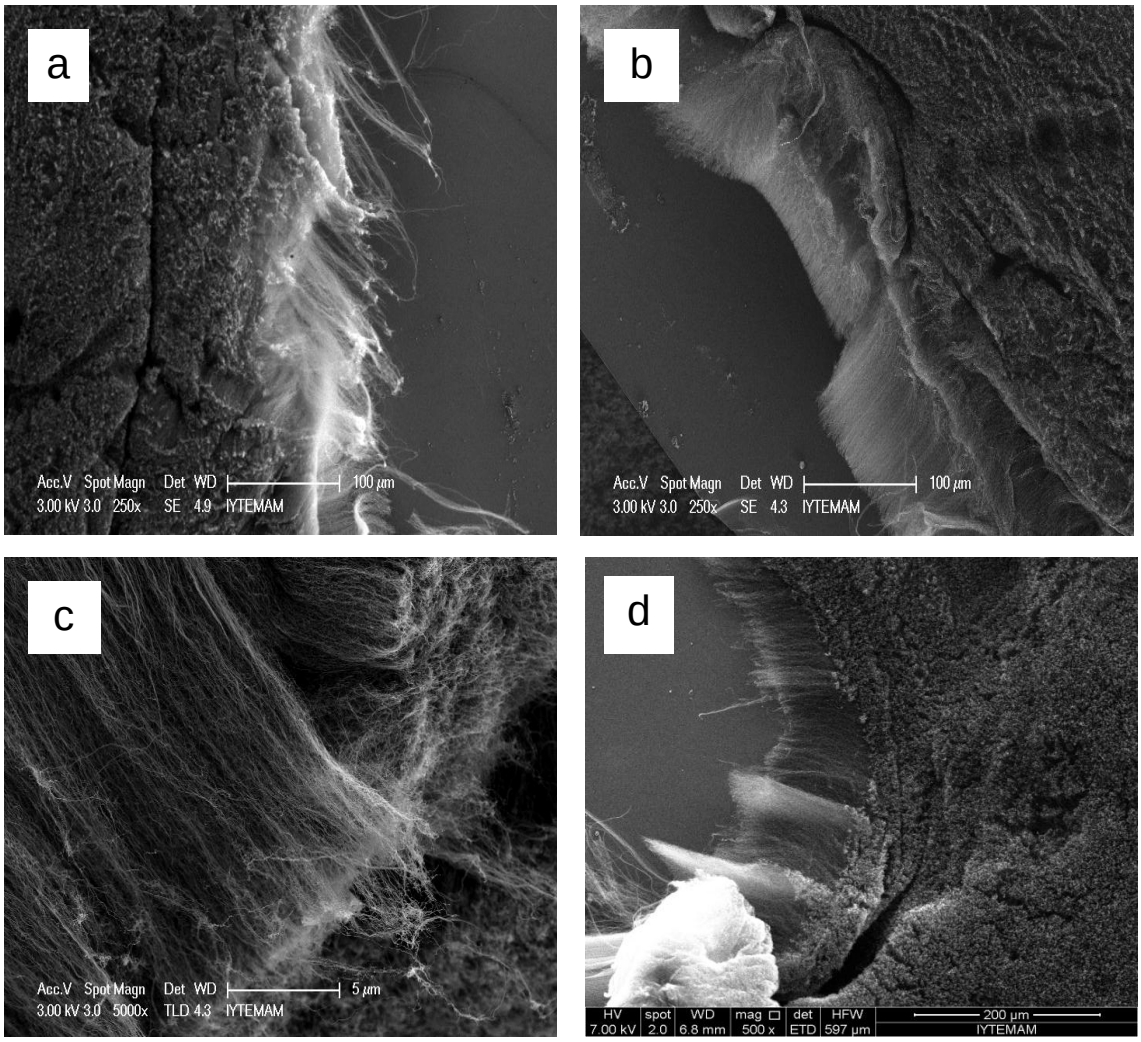

Figure 5.11. The growth in the presence CO_2 at 760 ^oC a) H_2:15 min., CO_2:5 min. b) H_2:15 min., CO_2:10 min., c) H_2:15 min., CO_2:2min. d) H_2:15min., CO_2:5min.

5.1.3. The Role of O_2 for Effective CNT Growth

The influence of O_2 on effective CNT growth was investigated by utilizing different pretreatment time and different O_2 levels. Pretreatment times of 15, 10, 5, 2 min. were studied. O_2 gas flows ratios in pretreatment and growth stages were studied as 5:1, 5:2, 2:2, 2:1, 2:0.5, respectively. It was observed from SEM analysis that the diameters of nanotubes increased with decreasing pretreatment time. This growth carried out by transforming the catalyst in the metal-oxide form to elemental form by removing the oxide with the help of H_2. As a result, we obtained small diameters at the pretreatment time of 15 min. in the presence of O_2. The diameters were changing between 6 nm and 8

nm. The diameters of the samples grown in pretreatment times of 10, 5, 2 min. were changing between 9 nm and 14 nm (Table 5.4).

We think that we obtained larger particles because film did not fully coalesce in short pretreatment times as shown in Figure 5.12. It was possible for metal-oxide film to reduce more effectively by increasing pretreatment time. The particles were smaller because the film effectively formed into clusters. Although we obtained small particle sizes in the presence of O_2, the density on the surface was low. This might be expected since O_2 during growth destroys defective nanotubes.

Table 5.4. The parameters studied with O_2 addition

Sample name	Pretreatment		CNT Growth			Mean Diameters of CNTS (nm)
	O_2 (sccm)	Time (min.)	C_2H_4 (sccm)	O_2 (sccm)	Time (min.)	
FeAlO14 CNT657	5	15	180	2	15	8.15
FeAlO14 CNT658	5	10	180	2	15	8.15
FeAlO14 CNT659	5	5	180	2	15	9.76
FeAlO14 CNT660	5	2	180	2	15	8.36
FeAlO14 CNT663	5	10	180	1	15	5.86
FeAlO14 CNT666	5	5	180	1	15	8.12
FeAlO14 CNT669	5	2	180	1	15	10.5
FeAlO14 CNT674	2	15	180	2	15	8.57
FeAlO14 CNT675	2	10	180	2	15	10.4
FeAlO14 CNT681	2	15	180	0.5	15	9.34

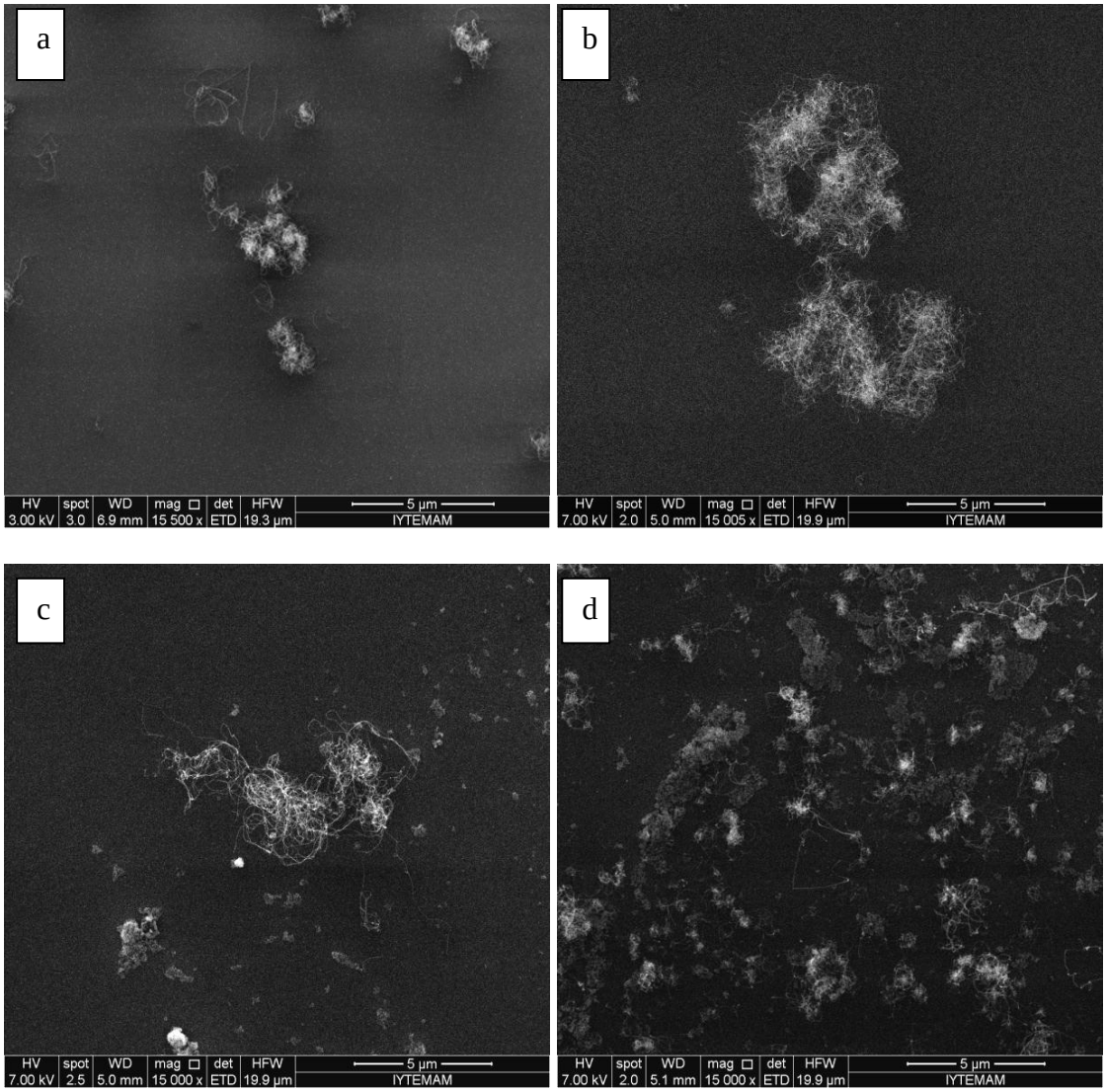

Figure 5.12. The growth with O_2 at 760°C a) CNT657,15 min. b) CNT658,10 min. c) CNT659, 5 min. d) CNT660, 2 min. e) CNT661, 15 min. f) CNT663, 10 min. g) CNT669, 2 min. h) CNT678, 15 min. , Magnifications: 15 000x

(cont. on next page)

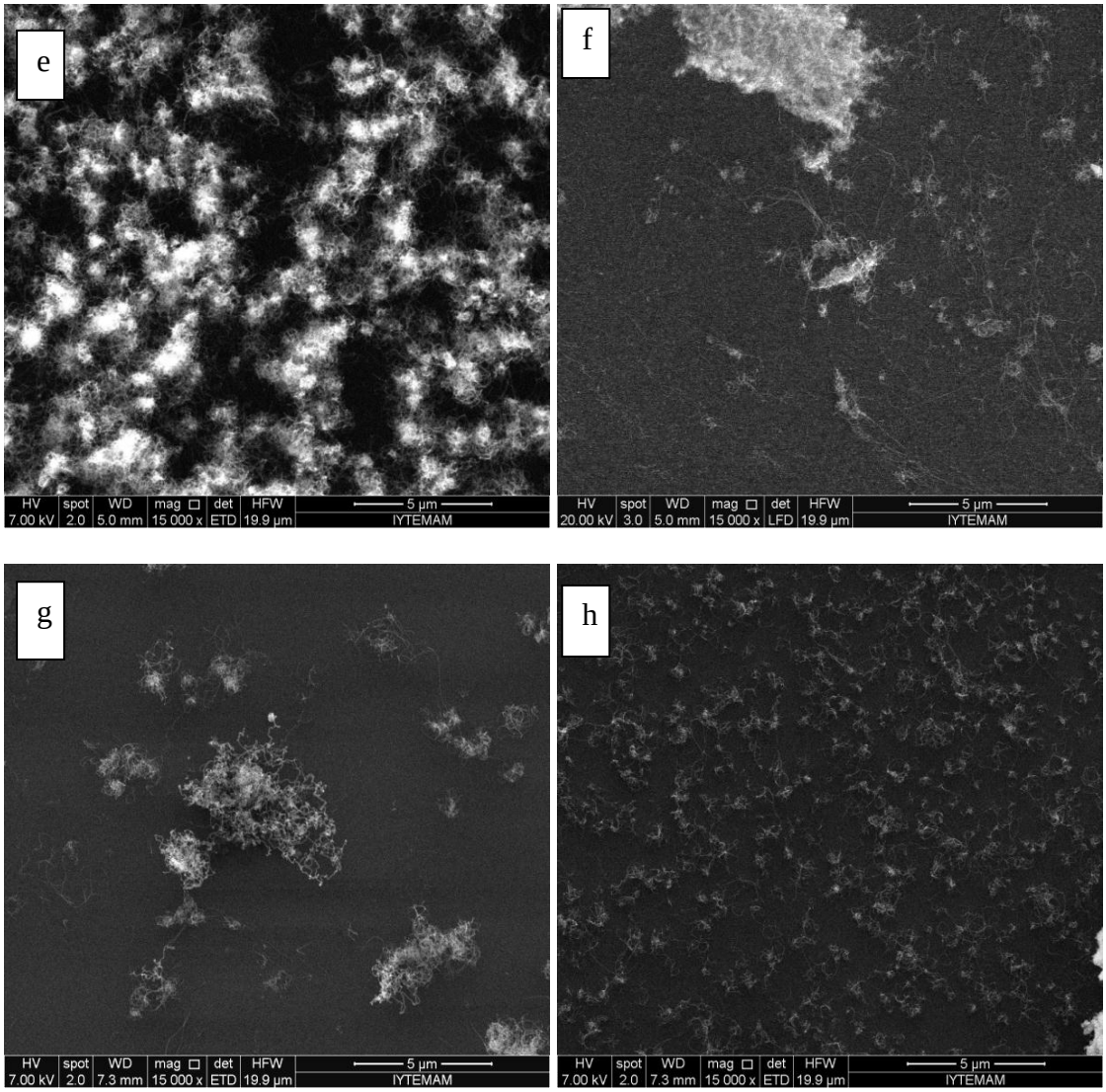

Figure 5.12. (cont.)

We also carried out experiments to study the influence of temperature in O_2-assisted CVD. Four different pretreatment times were studied at two different growth temperatures. Distribution of diameters obtained showed that catalyst nanoparticle sizes tightly controlled. By examining distribution of CNT diameters, we can say that low temperature was effective for CNT growth. At 740 ^oC growth, diameters of CNTs were between 5 nm and 20 nm and at 760 ^oC growth diameters of CNTs were between from 4 nm and 15 nm (Figure 5.13).

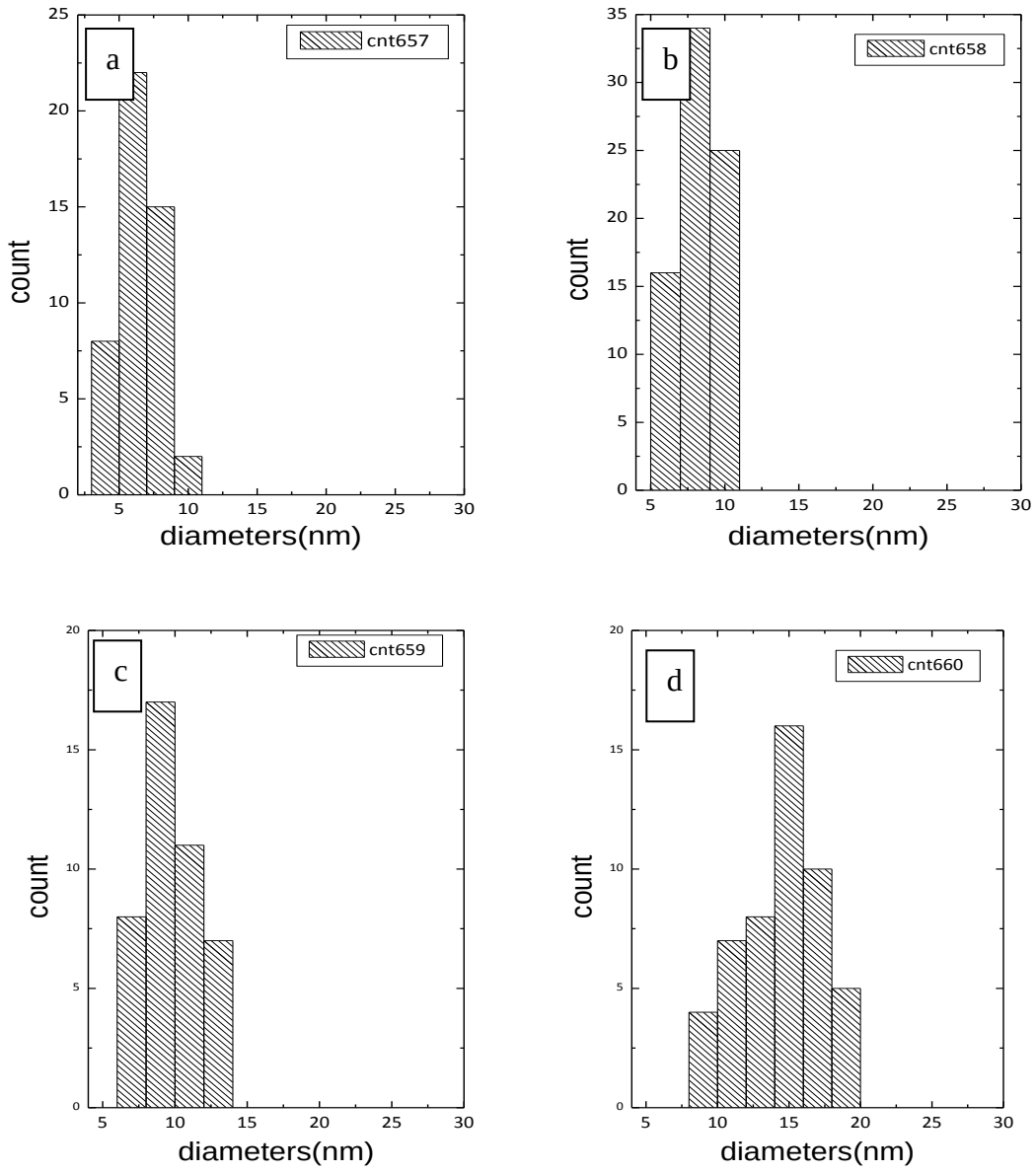

Figure 5.13. Diameter distributions of CNTs in the presence O_2 a) 740 ^{o}C, 15 min. b) 740 ^{o}C, 10 min. c) 740 ^{o}C, 5 min. d) 740 ^{o}C ,2 min. e) 760 ^{o}C, 15 min. f) 760 ^{o}C, 10 min. g) 760 ^{o}C, 5 min. h) 760 ^{o}C, 2 min.

(cont. on next page)

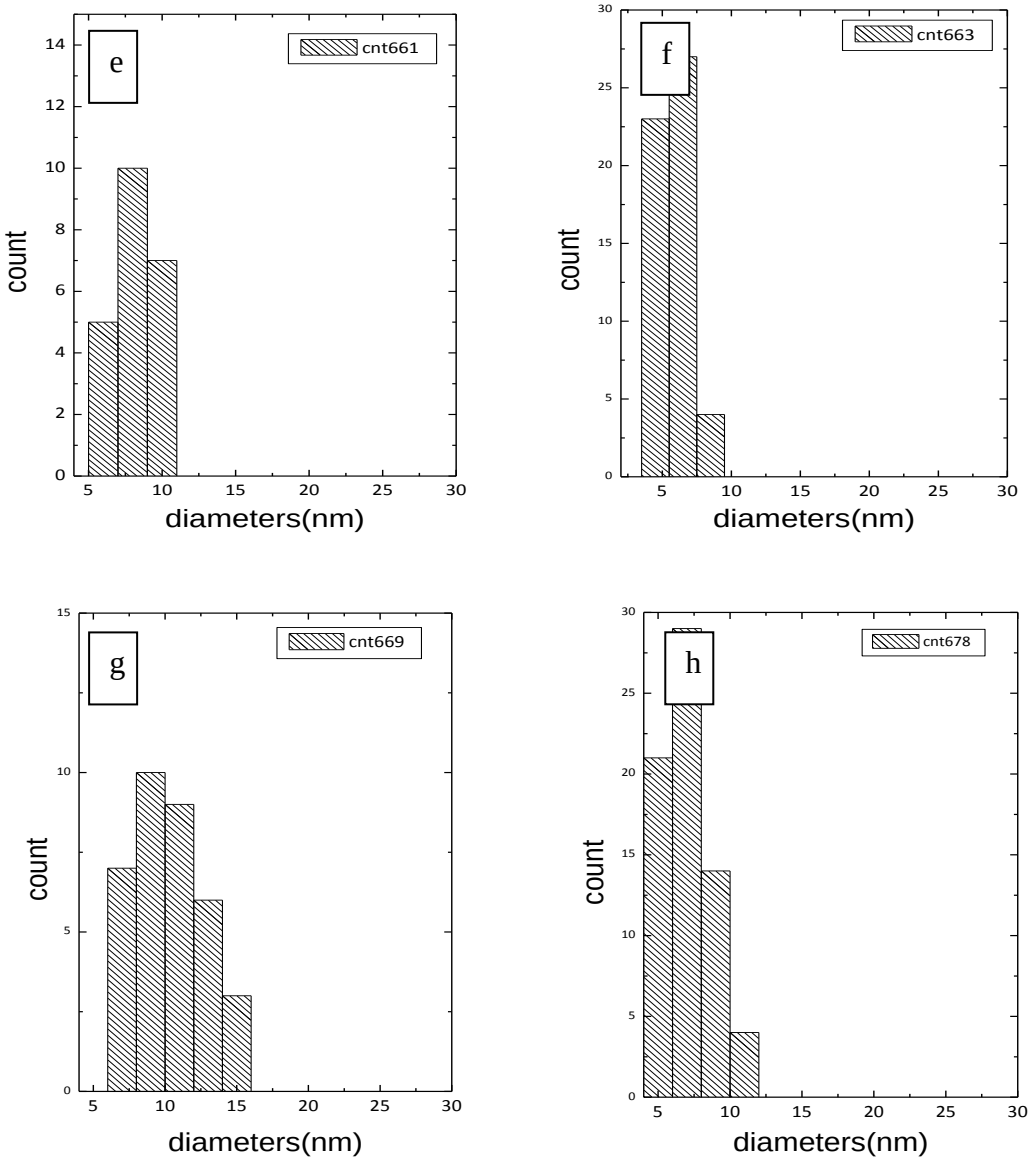

Figure 5.13. (cont.)

5.1.4. The Role of H_2O for Effective CNT Growth

H_2O is an essential ingredient to extend the lifetime of the catalyst during growth and, thus, leading to effective CNT growth. The effects of H_2O vapor for effective CNT growth under the same parameters were examined. The experiments were done only by studying the effect of H_2O amount. During the experiments, pretreatment time was kept at the constant value of 15 minutes and H_2O vapor levels

were varied. H_2O vapor levels were studied as 50 °C (A) / 50 °C (A), 50 °C (A) / 50 °C (B), 50 °C (B) / 50 °C (B), 50 °C (B)/ 50 °C (A), 60 °C(A) / 60 °C (A), 60 °C (A) / 60 °C (B), 60 °C (B) / 60 °C (B), 60 °C (B) / 60 °C (A), 70 °C (A) / 70 °C (A), 70 °C (A)/ 70 °C (B), 70 °C (B)/ 70 °C (B), 70 °C (B)/ 70 °C (A). B expresses much more H_2O and much more Ar than A, namely B is more diluted than A. The analysis showed that the best results were obtained at the growth utilizing H_2O at 60 °C (A) / 60 °C (A). CNT growth was dense and the mean diameters were kept at a narrow range as the samples grown with CO_2 as shown in Table 5.5.

Table 5.5. The parameters and mean diameters in the presence H_2O vapor
(H_2O (p): H_2O amount during pretreatment time)
(H_2O (g): H_2O amount during growth time)

Sample	Temperature (°C)	Pretreatment (min.)	H_2O(p)/ H_2O(g) (°C)	Mean diameter (nm)
FeAlO14 CNT693	760	15	60°C(A)/ 60°C(A)	7.01
FeAlO14 CNT696	760	15	60°C(A)/ 60°C(B)	7.47
FeAlO14 CNT699	760	15	60°C(B)/ 60°C(A)	8.04
FeAlO14 CNT700	760	15	60°C(B)/ 60°C(B)	6.80
FeAlO14 CNT701	760	15	50°C(A)/ 50°C(A)	7.60
FeAlO14 CNT702	760	15	50°C(A)/ 50°C(B)	9.11

When we examined SEM images as shown in Figure 5.14, the density of CNTs was higher compare to the samples studied with CO_2.

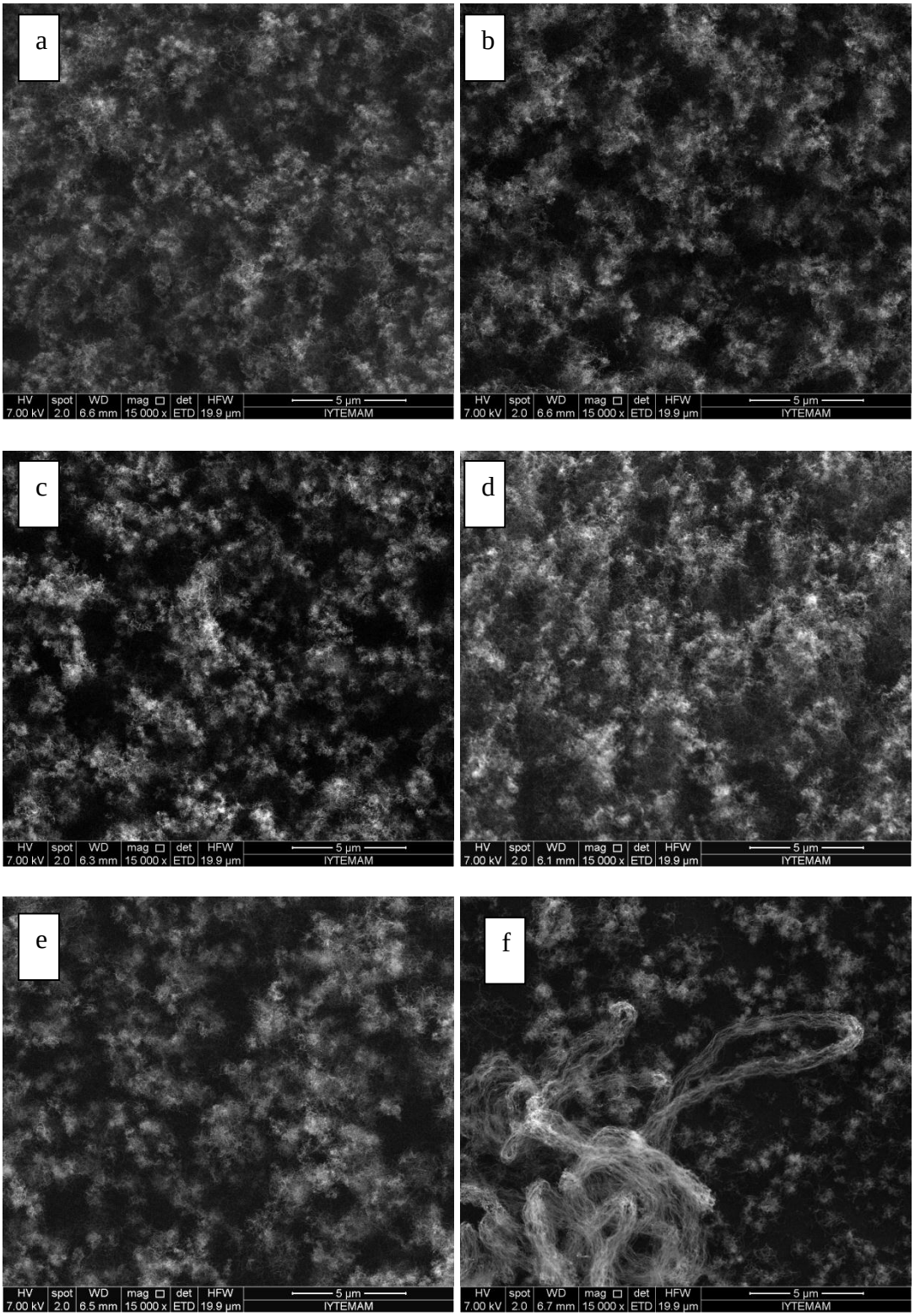

Figure 5.14. SEM images of CNTs grown in presence of H_2O at 760 ^oC a) CNT693 b) CNT696 c) CNT699 d) CNT700 e) CNT701 f) CNT702; Magnification: 15 000x

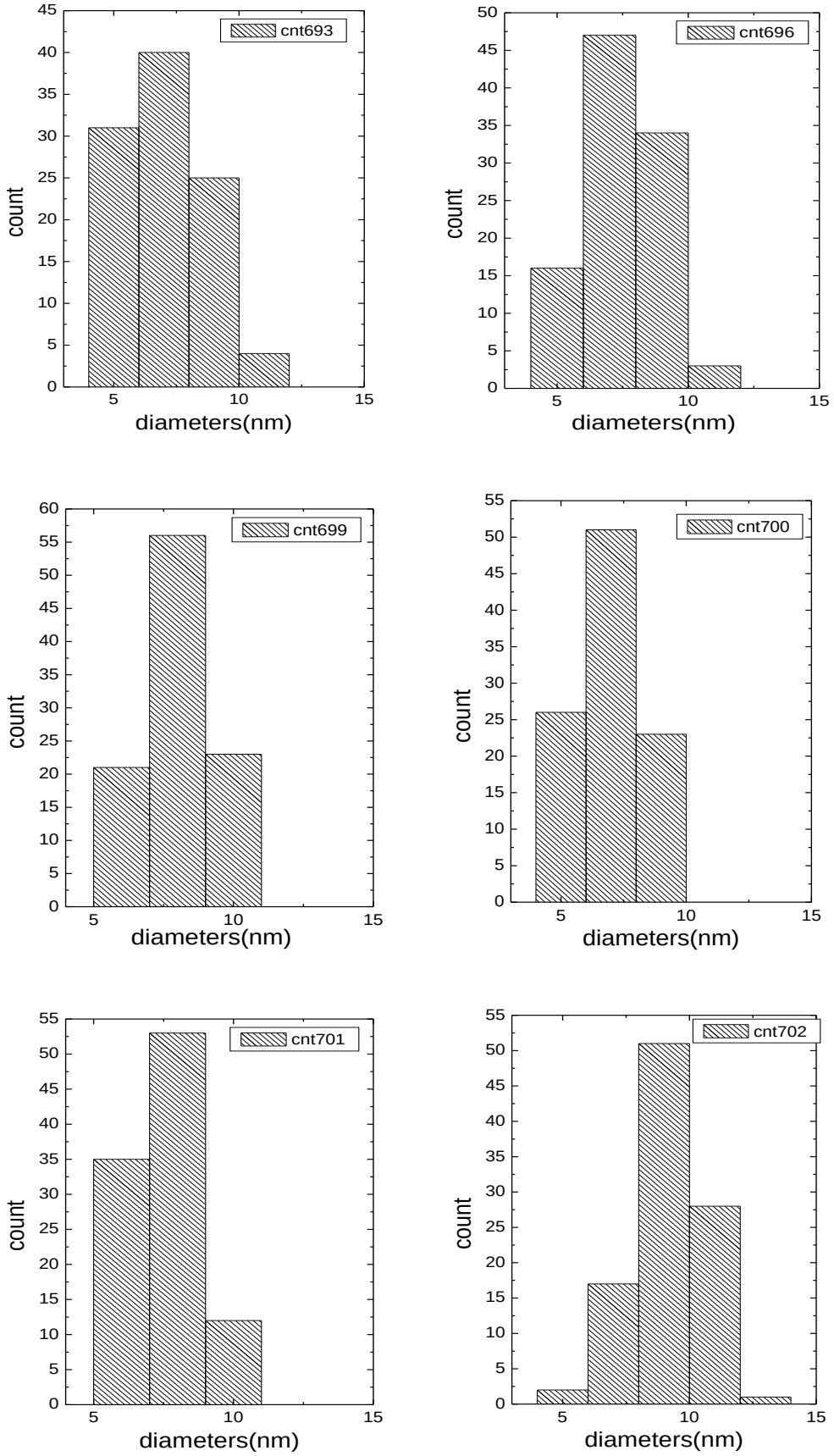

Figure 5.15. Diameter distributions of CNTs obtained in growths with the presence of H_2O

5.2. Raman Spectroscopy Results

Raman Spectroscopy with He-Ne laser with the excitation wavelength of 632.8 nm was used to observe the quality of CNTs and to find their types. The so-called G-line is a characteristic feature of the graphitic layers and corresponds to the tangential vibration of the carbon atoms at nearly ~1580 cm^{-1}. The second characteristic mode is a typical sign for defective graphitic structures (D-line) at nearly ~1335 cm^{-1}. The comparison of the ratios of these two peaks intensities gives a measure of the quality of the bulk samples. In addition, there is a third mode, called the radial breathing mode (RBM) which is very sensitive to the diameter of SWCNT and DWCNT.

The comparison of the ratios of these two peaks gives a measure of quality of the samples. In Figure 5.16, Disordered MWCNTs signal coming from the sample is shown. And also, the intensity of D line was bigger than the G-line intensity which indicated that there were defects in the structure of CNTs and these CNTs indicated metallic behavior. If these two bands have similar intensities, it is indication of a high quantity of structural defects.

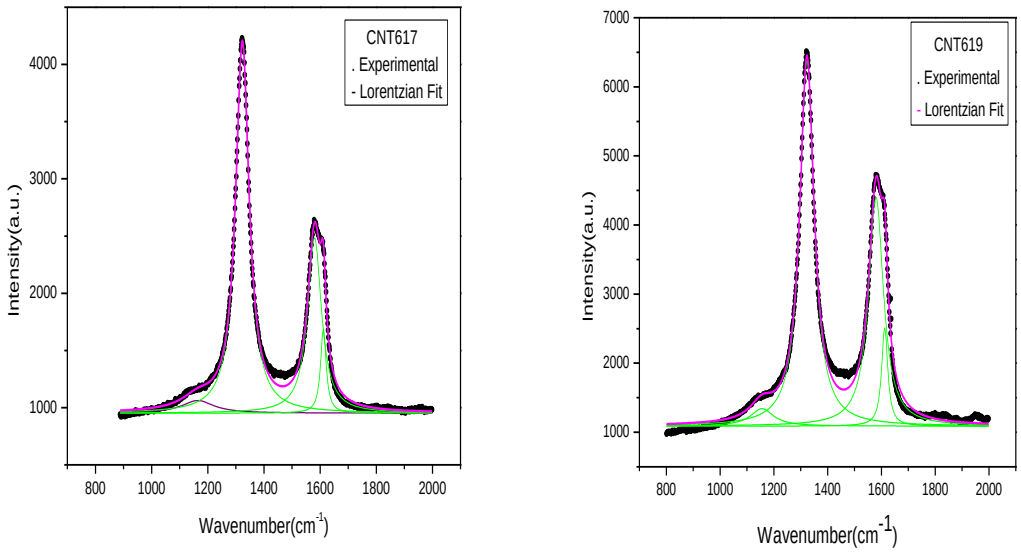

Figure 5.16. Raman analyses of CNTs a) CNT617, b) CNT619, c) CNT631, d) CNT639

(cont. on next page)

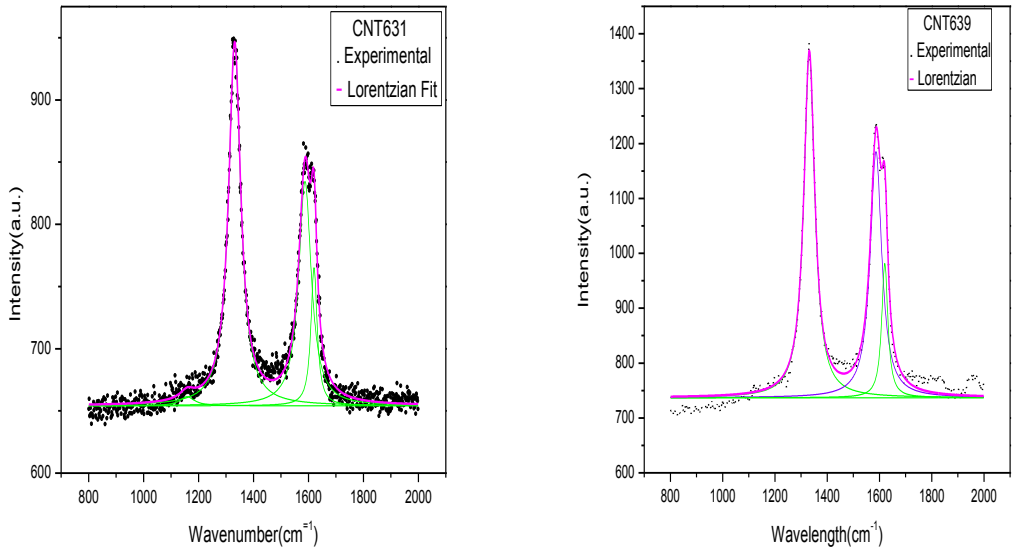

Figure 5.16. (cont.)

5.3. Statistical Analysis of All Samples

When standard deviations (Figure 5.17a) and standard errors (Figure 5.17b) of the mean diameters were analyzed us growth sequence (CNT number) of all samples grown by utilizing oxidizers, CNT diameters were kept at narrow range. Standard deviations of all patterns are seen to be ranging from 1-2 nm. In addition, standard error of all the mean of the diameters was very small.

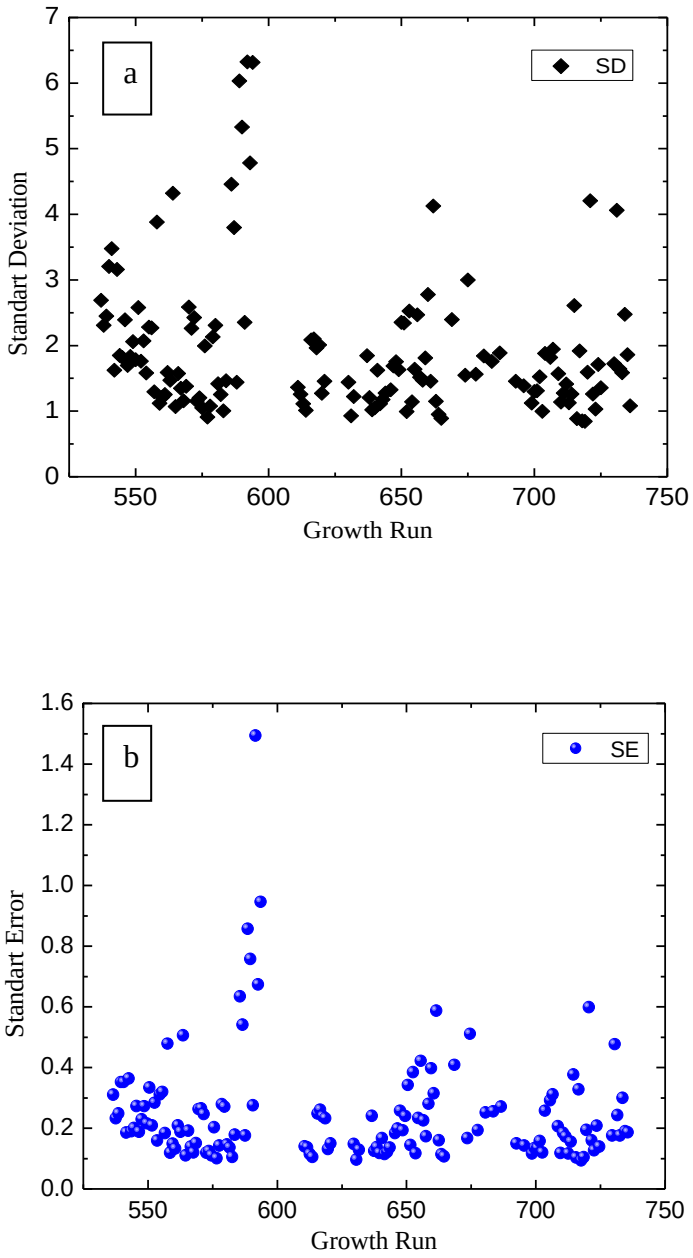

Figure 5.17. a) Standard deviation b) Standard error as CNT sequence of the samples grown by utilizing the oxidizers

Kurtosis value determines sharp-pointedness (optimal positive value) or flatness (optimal negative value) of distribution. For example, kurtosis of Gauss distribution that is skew neither right nor left is zero. When we look kurtosis value variation of CNT sequence (Figure 5.18a), values were generally seen to be between 1 and -1. There are few smaller values (three occurances) than -1, whereas there are more values with kurtosis value larger than +1 and, thus, explaining narrow distributions. While diameter

distributions are necessary for resembeling Gauss distribution is normally expected, these high positive kurtosis values were indication that CNT diameters were wihin narrow range of mean diameters. These results pointed that diameter distributions can be kept at very narrow range. In addition, when we looked at how skewness changed with growth sequence, all of distributions were observed to be skewed right (Figure 5.18 b). Right skewness is indication of Log-Normal instead of Normal distributions of CNT diameters. Similar observations were always seen catalyst particle distributions.

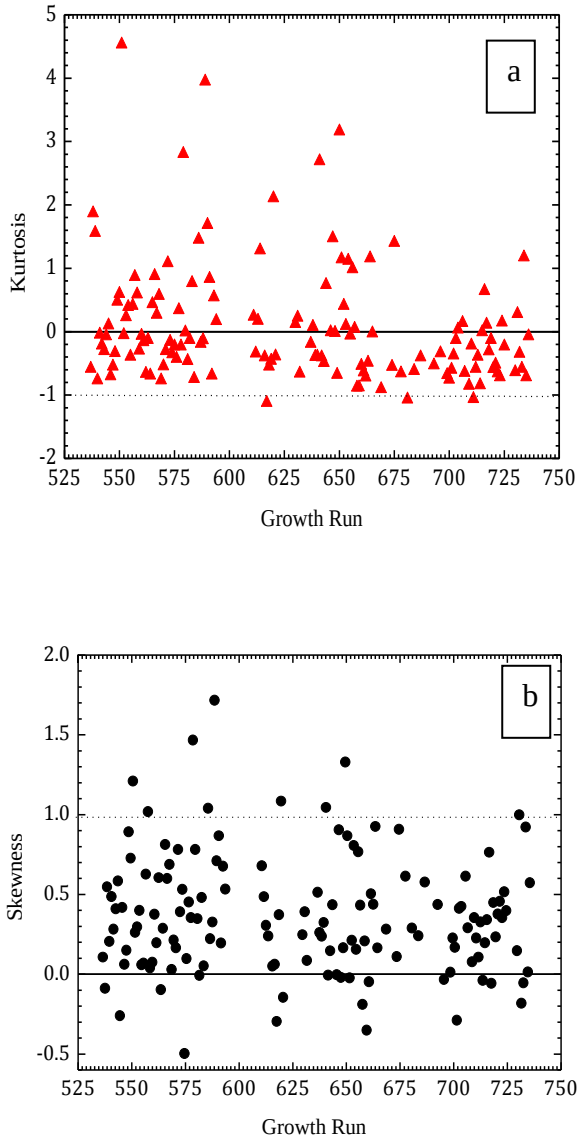

Figure 5.18. a) Kurtosis variations b) Skewness variations with CNT sequence of the samples grown by using oxidizers

Once we investigated how the mean diameters of CNTs change with growth sequence (Figure 5.19), diameters of the samples grown in the presence of CO_2 is orderly seen to decrease 5-7 nm range from around 13 nm. Other than first few samples, the mean diameters of samples with CO_2 were observed to changing between 5-7 nm, however, diameters of some samples were abruptly increasing. In general, diameters increased fast with the addition of oxidizers with both pretreatment and growth amount ratio of 2/2 sccm and, similarly, standard deviation was increasing as well. Moreover, diameters were larger with the addition of oxidizers during both pretreatment of 10 sccm and growth of 1 sccm than the other samples. The mean diameters of CNT growth utilized H_2O and O_2 as the oxidizers were within larger range, changing 6-11 nm range. The areal density of CNT growth with addition of O_2 was lower than CO_2 and H_2O.

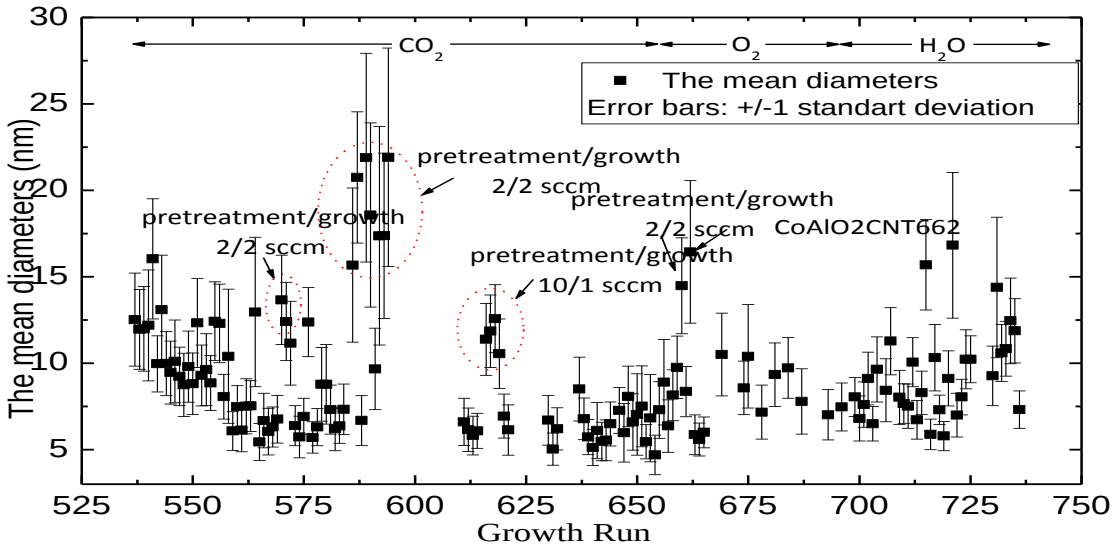

Figure 5.19. Variations of mean diameters with CNT sequence of the samples grown by using the oxidizers

CHAPTER 6

CONCLUSION

We demonstrated here the ability to optimize the process of growing diameter controlled carbon nanotubes. From analysis completed, the catalyst particle sizes were seen to accurately controlled via oxidizer gases using different pretreatment times. Especially CO_2 presented the best results obtained when we compare those obtained with O_2 and H_2O. It can be said that oxidizers help to keep catalyst particle distribution in narrow range during nucleation duration by looking at CNT diameter distribution and standard deviation. In addition, the data obtained from the effects of temperature on CNT growth was analyzed. Systematic ways of obtaining controlled-nanoparticles from catalyst film in order to grow effective CNT was presented with oxidizers gases.

We observed that diameter distributions of all the samples were similar to Log-Normal distribution as results of the extensive statistical analysis. CNT diameters were controlled within narrow range and CNT density was lower in the experiments done with O_2. This method is an effective way of keeping metal catalyst sizes a narrow range and thus resulting in narrow diameters of CNTs, therefore, resulting an effective production of CNTs. We believe that the ability to exert a profound degree of control over diameters of carbon nanotubes will facilitate the study of fundamental properties and development of new applications.

REFERENCES

Baddour, C. and C. Briens. 2005. Carbon Nanotube Synthesis. *Internation Journal of Chemical Reactor Engineering* 3:20-22

Baker, R.T.K., M.A. Barber, P.S. Harris, F.S. Feates, and R.J. Waite. 1972. Nucleation and growth of carbon deposits from the nickel catalyzed decomposition of acetylene. *Journal of Catalysis* 26:51-62.

Belin, T., Epron F. 2005. Characterization methods of carbon nanotubes. *Materials Science and Engineering* 119:105-118.

Bethune, D.S., C.H. Kiang, M.S. Vries, G. Gorman, R. Savoy, J. Vazquez, and R.Beyers. 1993. Cobalt-catalyzed growth of CNTs with single atomic layer walls. *Nature* 363:605-607.

Cho, Y.S., G.S. Choi, S.Y. Hong, and D. Kim. 2002. Carbon nanotube synthesis using a magnetic fluid via thermal chemical vapor deposition. *Journal of Crystal Growth* 243:224-229.

Cui, H., O. Zhou, and B.R. Stoner. 2000. Deposition of aligned bamboo-like carbon nanotubes via microwave plasma enhanced chemical vapor deposition. *Journal of Applied Physics* 88(10):6072-6077.

Cui, H., G. Eres, J.Y. Hawe. 2003. Growth behavior of carbon nanotubes on multilayered metal catalyst film in CVD. *Chemical Physics Letters* 374:222-228.

Dai H. 2002. Carbon nanotubes: opportunities and challenges. *Surface Science* 500:218-241.

Deck, C.P. and K. Vecchio. 2006. Prediction of Carbon nanotube growth success by the analysis of carbon-catalyst binary phase diagrams. *Carbon* 44:267-275.

Dresselhaus, Mildred S., Gene Dresselhaus, and Phaedon Avouris, eds. 2001. Carbon nanotubes: synthesis, structure, properties, and applications. Berlin: Springer Publishers.

Duesberg, G.S., A.P. Graham, M. Liebau, R. Seidel, E. Unger, F. Kreupl, and W.Hoenlein. 2003. Growth of isolated carbon nanotubes with lithographically defined diameter and location. *Nano Letters* 3(2):257-259.

Fonseca, A., K. Hernadi, J.B. Nagy, D. Bernaerts, and A.A. Lucas. 1996. Optimization of catalytic production and purification of buckytubes. *Journal of Molecular Catalysis A: Chemical* 107:159-168.

Futaba, D. 2006. Shape-engineerable and highly densely packed single-walled carbon nanotubes and their application as super-capacitor electrodes. *Nature Materials* 5(12):987-994.

Gassell, M. 1999. Large Scale CVD Synthesis of Single Walled Carbon Nanoyubes. *Journal Physics Chemistry* 103:6484-6492.

Guo, T., P. Nikolaev, A. Thess, D.T. Colbert, and R.E. Smalley. 1995. Catalytic growth of single-walled nanotubes by laser vaporization. *Chemical Physics Letters* 243:49-54.

Hata K., D. Futaba, K. Mizuno, T. Namai, M. Yumura and S. Iijima. 2004. Water-assisted highly efficient synthesis of impurity free SWCNT. *Science* 306:1362-1365.

Hernadi, K., A. Fonseca, J.B. Nagy, D. Bernaerts, A. Fudala, and A.A. Lucas. 1996. Catalytic synthesis of carbon nanotubes using zeolite support. *Zeolites* 17:416-423.

Huang J., Q. Zhang, M. Zhao and F. Wei. 2009. Process intensification by CO_2 for high quality carbon nanotube forest growth: Double-walled carbon nanotubes convexity or single-walled carbon nanotube bowls? *Nano Research* 2:872-881.

Iijima, S. 1991. Helical microtubules of graphitic carbon. *Nature* 354:56-58.

Iijima, S. and T. Ichihashi. 1993. Single-shell carbon nanotubes of 1 nm diameter. *Nature* 363:603-605.

Ivanov, V., J. B. Nagy, P. Lambin, A. Lucas, X.F. Zhang, and D. Bernaerts. 1994. The study of carbon nanotubules produced by catalytic method. *Chemical Physics Letters* 223:329-335.

Ivchenko, E.L. and B. Spivak. 2002. Chirality effects in carbon nanotubes. *Physical Review B* 66(15):155404-155413.

Journet, C. and P. Bernier. 1998. Production of carbon nanotubes. *Applied Physics A* 67:1-9.

Kataura, H., Y. Kumazawa, Y. Moniwa, Y. Ohtsuka. 2000. Diameter control of single walled carbon nanotubes. *Carbon* 38(11-12):1691-1697.

Kiang, C. H. 2000. Carbon rings and cages in the growth of single-walled carbon nanotubes. *Journal of Chemical Physics* 113(11):4763-4767.

Klinke,C., J.-M. Bonard, and K. Kern. 2001. Comparative study of the catalytic growth of patterned carbon nanotube films. *Surface Science* 492:195-201.

Kroto, H.W., J.R. Heath, S.C. O'Brien, R.F. Curl, R.E. Smalley. 1985. C60: buckminsterfullerene. *Nature* 318:162-163.

Kukovecz, A., Z. Kónya, N. Nagaraju, I. Willems, A. Tamási, A. Fonseca, J.B. Nagy, I.Kiricsi. 2000. Catalytic synthesis of carbon nanotubes over Co, Fe and Ni

containing conventional and sol–gel silica–aluminas. *Physical Chemistry Chemical Physics* 2:3071-3076.

Lee, C. J., J. Park, and J.A. Yu. 2002. Catalyst effect on carbon nanotubes synthesized by thermal chemical vapor deposition. *Chemical Physics Letters* 360:250-255.

Li, X., X. Zhang, L. Ci, R. Shah, C. Wolfe, S. Kar, S. Talapatra and P. Ajayan.2008. Air-assisted growth of ultra-long carbon nanotube bundles, *Nanotechnology* 19: 455-609.

Moisala, A., A.G. Nasibulin, and E.I. Kapauppinen. 2003. The role of metal nanoparticles in the catalytic production of single-walled carbon nanotubes. *Journal of Physics: condensed matter* 15:3011-3035.

Oberlin A, M. Endo, T. Koyama. 1976. Filamentous growth of carbon through benzene decomposition. *Journal of Crystal Growth* 32:335-349.

Pan, S.S., Z.W. Xie, B.H. Chang, L.F. Sun, W.Y. Zhou, and G. Wang. 1999. Direct growth of aligned open carbon nanotubes by chemical vapor deposition. *Chemical Physics Letters* 299:97-102.

Park J.B, G.S. Choi, Y.S. Cho, S.Y. Hong, D. Kim, S.Y. Choi, J.H. Lee, K. Cho. 2002. Characterization of Fe-catalyzed carbon nanotubes grown by thermal chemical vapor deposition. *Journal of Crystal Growth* 244:211-217.

Popov, V.N.2004. Carbon nanotubes: properties and applications. *Materials Science and Engineering Reports* 43:61-102.

Qingwen, L., Y. Hao, C. Yan, Z. Jin, L. Zhongfan. 2002. A scalable CVD synthesis of high purity single walled carbon nanotubes with porous MgO as support material. *Journal of Materials Chemistry* 12:1179-1183.

Radushkevich LV, V.M. Lukyanovich. 1952. O strukture ugleroda, obrazujucegosja priTermiceskom razlozenii okisi ugleroda na zeleznom kontakte. *Zurn Fisic Chim* 26:88-95.

Reich, S., C. Thomsen, and J. Maultzsch. 2004. Carbon *nanotubes: basic concepts and physical properties*. Berlin: Wiley-VCH.

Richardson, J. T. 1989. Principles and catalyst development. *New York: Plenum Press.*

Rotkin, Slava V. and Shekhar Subramoney, eds. 2005. Applied physics of carbon nanotubes: fundamentals of theory, optics, and transport devices. *New York: Springer Publishers.*

Saito, R., M. Fujita, G. Dresselhaus, M.S. Dresselhaus. 1992. Electronic structure of chiral graphene tubules. *Applied Physics Letters* 60(18):2204-2207.

Saito Y, M. Okuda, N. Fujimoto, T. Yoshikawa, M. Tomita, T. Hyashi. 1994. Single wall carbon nanotubes growing rapidly from Ni fine particles formed by arc evaporation. *Japan Journal of Applied Physics Part 2- Letters* 33:526-529.

Salvetat, G. Andrew, D. Briggs, J.M. Bonard, Revathi, R. Bacsa, Andrzej, J. Kulik, T. Stockli, N.A. Burnham, L. Forro. 1998. Physical Review Letters 82.

Thostenson, E.T., Z. Ren, and T.W. Chou. 2001. Advances in the science and technology of carbon nanotubes and their composites: a review. *Composites science and Technology* 61:1899-1912.

Venegoni, D., P. Serp, R. Feurer, Y. Kihn, C. Vahlas, and P. Kalck. 2002. Parametric study for the growth of carbon nanotubes by catalytic chemical vapor deposition on a fluidized bed reactor. *Carbon* 40:1799-1807.

Walker, P.L., F. Rusinko, L.G. Austin. 1959. Gas reactions of carbon. *Advances in Catalysis* 11:133-221.

Weifeng, L., W. Cai, L.Yao, X. Li, Z. Yao. 2003. Effects of methane partial pressure on synthesis of single walled carbon nanotubes by chemical vapor deposition. *Journal of Materials Science* 38:3051-3054.

Yacaman, M.J., M.M. Yoshida, L. Rendon, and J.G. Santiesteban. 1993. Catalytic growth of carbon microtubules with fullerene structure. *Applied Physics Letters* 62:202-207.

Yudasaka, M., R. Kikuchi, T. Matsui, O. Yoshimasa, and S. Yoshimura. 1995. Specific conditions for Ni catalyzed carbon nanotube growth by chemical vapor deposition. *Applied Physics Letters* 67:2477-2482.

Yudasaka, M., R. Kikuchi, Y. Ohki, E. Ota, and S. Yoshimura. 1997. Behavior of Ni in carbon nanotube nucleation. *Applied Physics Letters* 70:1817-1821.